Lithospheric structure beneath the Mesozoic (~140 – ~110 Ma) Chilwa Alkaline Province (CAP) in southern Malawi and northeastern Mozambique

By

VICTOR NYALUGWE

Bachelor of Arts/Science in Geology

University of Malawi-Chancellor College

Zomba, Malawi

2008

Submitted to the Faculty of the
Graduate College of the
Oklahoma State University
in partial fulfillment of
the requirements for
the Degree of
MASTER OF SCIENCE
May, 2018

Lithospheric structure beneath the Mesozoic (~140 – ~110 Ma) Chilwa Alkaline Province (CAP) in southern Malawi and northeastern Mozambique

Thesis Approved:

Dr. Mohamed G. Abdel Salam

Thesis Adviser

Dr. Estella A. Atekwana

Dr. Jack Pashin

ACKNOWLEDGEMENTS

I would like to express my sincere gratitude to my advisors Dr. Mohamed G. Abdelsalam and Dr. Estella A. Atekwana for their supervision, encouragement and coaching. This work is made possible due to their continued help. I also express my thanks to Dr. Pashin who was one of the committee members for his recommendations in improving my thesis. Dr Andrew Kutumwehe as well as Dr. Daniel A. Lao-Davila needs to receive very special thanks for their major contributions and inputs towards this work too.

Malawi Government under Mining Governance and Growth Support Project through World Bank Loan funded this project in conjunction with GEEMAP-a project funded by the French Government. The main goal for these projects was to enhance mineral exploration and other geological related information of which the country still deems to have gaps hence the goal of this work too.

I cannot forget to thank my fellow students such as Mercy Achang, Luel Emishaw, Tadesse Alemu, Steven Johnston, Micah Mayle, and Jeannot Goussi for their tremendous help during my study period.

Special thanks have to be sent to my family members who are my Father and Mom-Mr. and Mrs. Nyalugwe; brothers and sisters as well as Olive, Desire, Flossy and Comfort for their endless support, encouragement, prayers and everything positive towards me. Charles Missi receives my special thanks too for the all through study time partner who we have gone together through ups and downs till to this positive end.

Name: VICTOR NYALUGWE

Date of Degree: MAY, 2018

Title of Study: **Lithospheric structure beneath the Mesozoic (~140 – ~110 Ma) Chilwa Alkaline Province (CAP) in southern Malawi and northeastern Mozambique**

Major Field: GEOLOGY

Abstract

This work investigates the lithospheric structure beneath the Mesozoic (~140 – ~110 Ma) Chilwa Alkaline Province (CAP) in southern Malawi and northeastern Mozambique using aeromagnetic and satellite gravity data (the World Gravity Model 2012 (WGM 2012). The CAP is a granite, syenite, nepheline syenite, and basanite province with minor intrusions of carbonatite bodies. It intrudes the Precambrian terranes of the Southern Irumide belt and the Unango complex. It is located on the northeastern margin of the Mesozoic Shire graben and on the southeastern edge of the Cenozoic Malawi rift, which is considered the southernmost segment of the Western Branch of the East African Rift System (EARS). Some of the CAP's intrusive bodies are clearly offset by the border normal faults of the Malawi rift. Previous petrographic, geochemical and isotopic studies have suggested that the CAP is underlain by a thinned sub-continental lithospheric mantle (SCLM) possibly due to the Mesozoic Karoo rifting event. Hence, mantle magmatic source has been favored as an origin for the CAP. However, melting of a thickened continental crust cannot be ruled out for the origin of the CAP as has been suggested for several other alkaline intrusions. In this study: (1) Edge enhancement of the aeromagnetic data showed the CAP to be defined by circular and overlapping magnetic anomalies typical of hypabyssal nested igneous ring complexes. (2) Three-dimensional (3D) Voxi modeling and magnetic susceptibility analysis of the aeromagnetic data covering selected CAP's intrusive bodies showed that these were emplaced at an average depth of ~ 4 km. (3) Upward continuation of the WGM 2012 Bouguer gravity anomalies suggested that the CAP was sourced from possibly deeper magma chambers now preserved as broad batholiths at ~4 km to~6 km depth. (4) Two-dimensional (2D) radially-averaged power spectral analysis of the WGM 2012 Bouguer gravity anomalies showed that the CAP is underlain by a thick crust (possibly due to mafic magmatic under-platting) where the Moho can be as deep as ~45 km. It also showed that the CAP is underlain by a relatively thin SCLM (possibly due to Mesozoic Karoo rift-related lithospheric stretching) where the asthenosphere-lithosphere boundary (LAB) can be as shallow as ~110 km. This work suggests that thinning of the SCLM might have allowed for the ascendance and decompression melting of the asthenosphere but also provided heat source (through mafic magmatic under-platting) to partially melt the lower crust to form the CAP from a mixed magma source and through caldera collapse mechanism. This model can be tested by additional geochemical and isotopic studies. This work highlights the importance of potential field data for imaging complex continental lithospheric structure. Understanding the lithospheric structure beneath the CAP is helpful in guiding future mineral exploration efforts because igneous ring complexes are important sites for the formation of economic mineralization zones.

TABLE OF CONTENTS

Figure Page

CHAPTER I

INTRODUCTION

A striking geological feature of the African continent is the presence of spectacular clusters of alkaline igneous intrusions often in the form of ring complexes (Bowden, 1985; Black and Lameyre, 1985; Vail, 1989; Abdelsalam et al., 2016). It has been observed that there are far more igneous ring complexes in Africa than in any other continent (Vail, 1989). It has also been shown that these alkaline rocks have intruded the African lithosphere throughout much of its geological history that spans the Paleoproterozoic (2000 Ma) to the Oligocene (25 Ma) (Black and Lameyre, 1985). It has also been shown that igneous ring complexes are often emplaced in clusters and hence referred to as migrating, overlapping, or nested igneous ring complexes. (O'Halloran, et al., 1985; Bonin et al., 2004; Abdelsalam et al., 2016). In Africa, the ~1.85 Ga Singo granite in Uganda is one of the oldest alkaline igneous intrusion which has been documented as a nested ring complex using aeromagnetic and satellite gravity data (Abdelsalam et al., 2016). Because of their well-defined geologic context, igneous ring complexes provide an unparalleled opportunity to evaluate the evolution of sub-volcanic magmatic systems and upper-crustal magma transfer (Johnson et al., 1999).

The mostly accepted model for the formation of igneous ring complexes is the caldera collapse model (Bonin et al., 2004; Abdelsalam, 2016). This model proposes that the collapse of the caldera usually occurs because of the emptying of magma chamber

beneath it. Emptying of the magma chamber occurs through the eruptions that take place on the flanks of the associated volcano and fissure system that extract magma from the chamber. The decrease in pressure in the magma chamber results in an increase in tensile stress, which in turns creates tensional fractures at the surface of the volcano. The higher the radius to the depth of the magma chamber, the higher the probability of forming the caldera. Once a critical tension is approached, the roof of the magma chamber collapses and this is referred to as caldron subsidence. In this case, the term collapse caldera refers to those volcanic depressions resulting from the sinking of the chamber roof into the magmatic reservoir due to the rapid withdrawal of magma during the course of an eruption (Bonin et al., 2004; Geyer et al., 2014; Abdelsalam et al., 2016). This explanation is applicable to all kinds of calderas, regardless of magma composition, tectonic setting, shape, size, or amount of subsidence (Geyer et al., 2014).

The first-order geodynamic evolution of igneous ring complexes can be summarized into three broad models: (1) Uprising of a mantle plume leading to rifting (Morgan, 1972; Gass et al., 1978). (2) Melting of a lower crust that was previously thickened during an orogenic event and subsequent gravitational collapse (Bonin, 2007). (3) Delamination of a sub-continental lithospheric mantle (SCLM) (Black and Liegeois, 1993; Abdelsalam et al., 2002; Avigad and Gvirtzman, 2009). It has also been suggested that lithospheric-scale, shear zone provide second- scale, shear zone provide second-order controls on the emplacement of the igneous ring complexes (Black and Lameyre, 1985; Moreau et al., 1994; Azzouni-Sekkal et al., 2003). These shear zones influence the

localization of aligned magmatic centers that show the relationship between deep-seated faulting and the emplacement of igneous ring structures. Examples of this model include the Borborema Province of northeast Brazil where Neoproterozoic granitoids and large-scale strike-slip shear zones are spatially associated, suggesting a genetic link between magma bodies and shear zones (Neves et al., 1995).

The Mesozoic Chilwa Alkaline Province (CAP) in southern Malawi and northern Mozambique (Figs. 1.1 – 1.4) is an excellent site to study the geodynamic evolution of igneous ring complexes. Previous petrographic, geochemical and isotopic studies suggest the presence of a thin SCLM beneath the CAP, possibly due to Mesozoic Karoo rifting event. Hence, mantle magmatic source has been favored as an origin for the CAP (e.g. Eby et al., 1998). However, melting of a thickened continental crust cannot be ruled out for the origin of the CAP as has been suggested for several alkaline intrusions (e.g. Bonin, 2007). Nonetheless, as in the case for many igneous ring complexes, no effort has been spent to systematically image the lithospheric structure beneath the CAP, from the surface to the lithosphere-asthenosphere boundary (LAB). This work makes advantage of the availability of remote sensing and potential field geophysical data to fill this knowledge gap. First, Landsat Thematic Mapper (TM), Shuttle Radar Topography Mission (SRTM) Digital Elevation Model (DEM) and filtered aeromagnetic data are used to map the surface and near-surface geometry of the CAP.

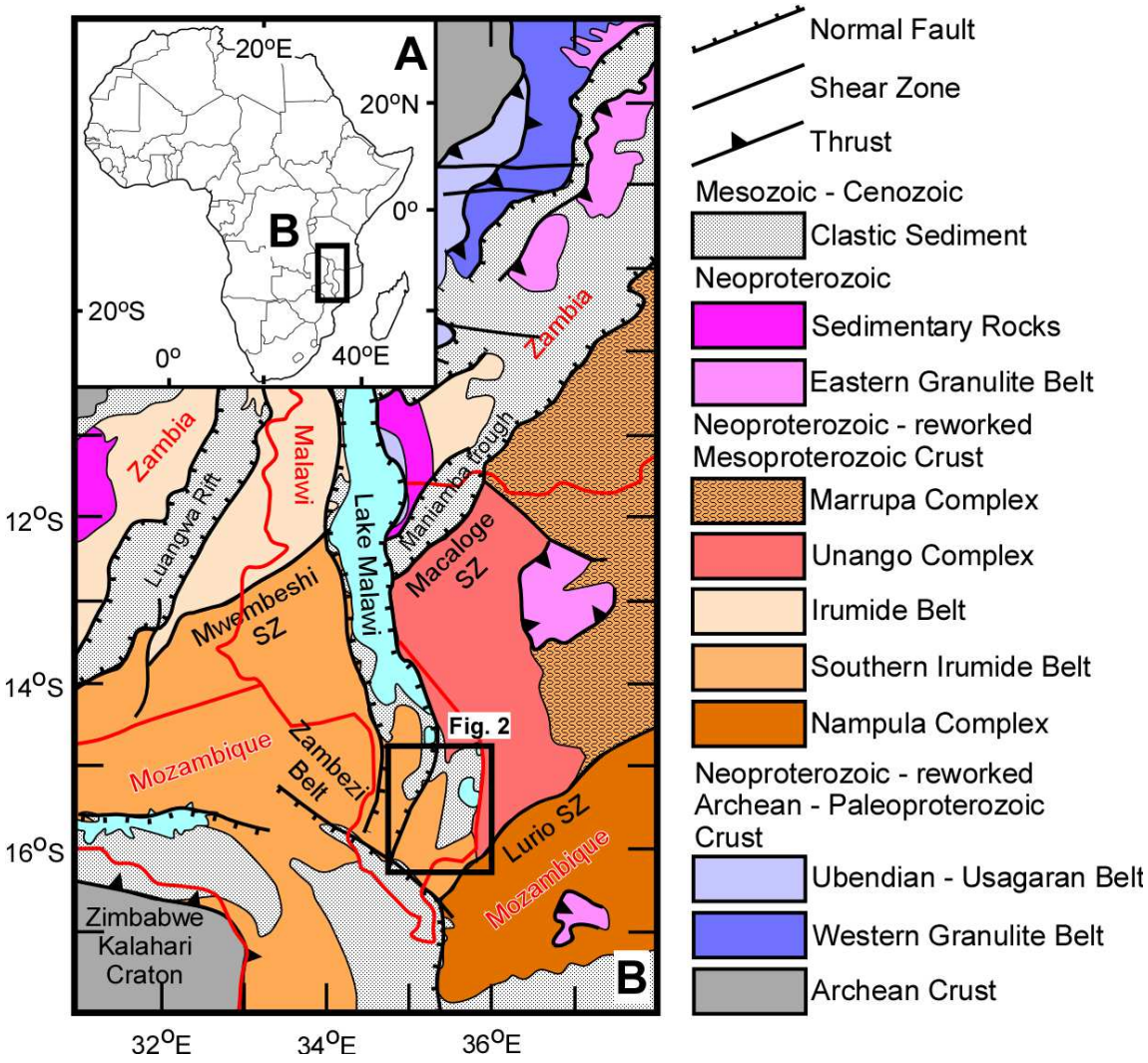

Figure 1.1: (A) Location of Malawi and the surrounding countries within Africa. (B) Regional tectonic map showing the exposures of the Precambrian and the Mesozoic - Cenozoic units around the Chilwa Alkaline Province (CAP). Modified after Fritz et al. (2013) and Laó –Dávila et al., (2015).The black rectangle shows the location of the study area.

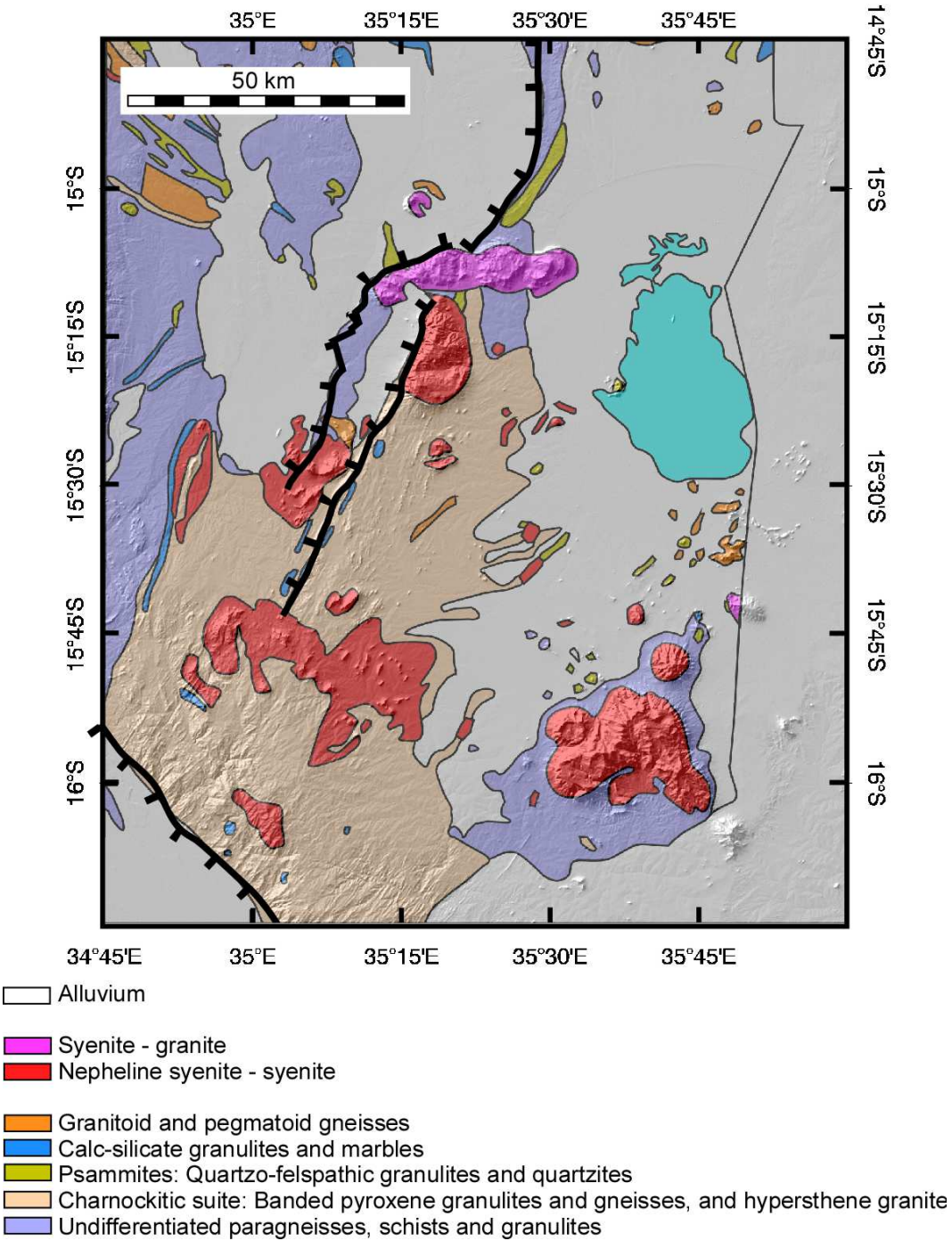

Figure 1.2: Geological map of the Chilwa Alkaline Province (CAP). Modified from the Malawi Geological Survey Map, 1995.

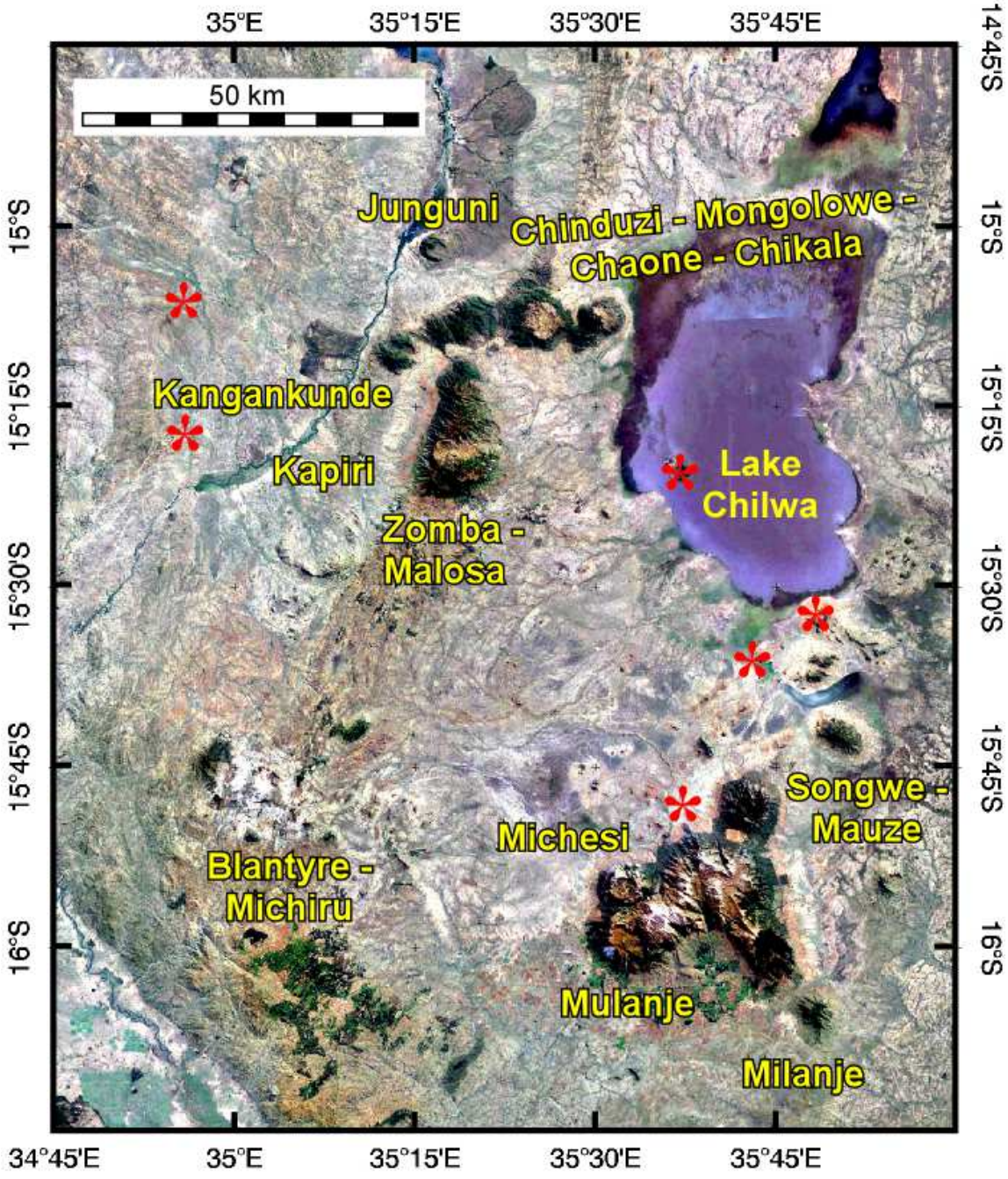

Figure 1.3: Natural color 3-2-1 (Red-Green-Blue – RGB) color combination Landsat Thematic Mapper (TM) image of the Chilwa Alkaline Province (CAP). The image is obtained from Google Earth Pro.

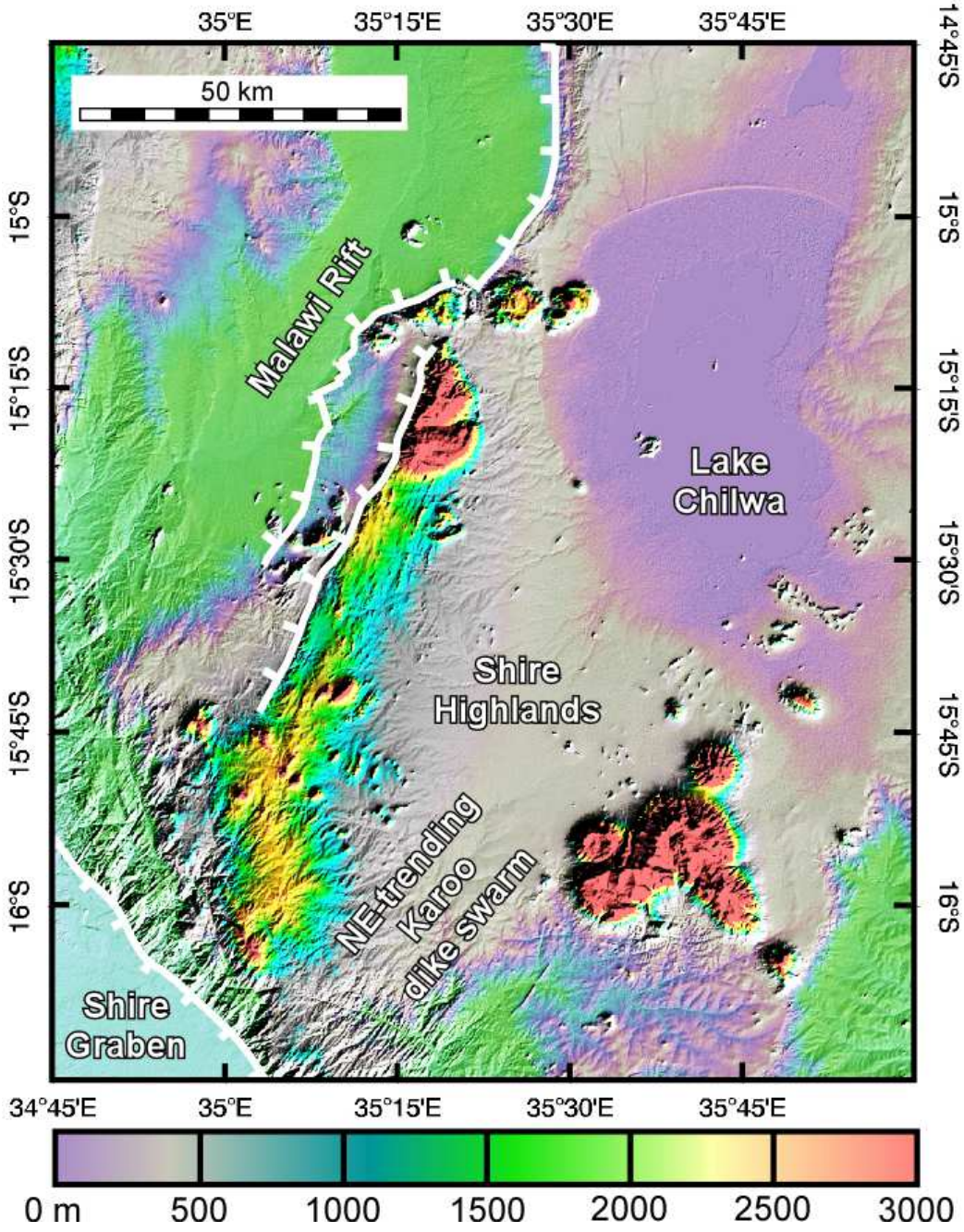

Figure 1.4: Shuttle Radar Topography Mission (SRTM) Digital Elevation Model (DEM) of the Chilwa Alkaline Province (CAP).

Second, three-dimensional (3D) Voxi modeling of the aeromagnetic data, magnetic susceptibility analysis, and upward continuation of the Bouguer gravity anomalies of the World Gravity Model 2012 (WGM 2012) are used to map the shallow depth magmatic sources of the CAP and possibly the underlying frozen magma chamber. Third, two-dimensional (2D) radially average power-spectral analysis (henceforth spectral analysis) of the WGM 2012 Bouguer gravity anomalies is implemented to map the depth to Moho and the LAB. Alkaline igneous provinces and carbonatites contain economic mineral deposits such as iron (Fe), Niobium (Nb), Rare Earth Elements (REE), Copper (Cu), phosphate, vermiculite, and nepheline. Therefore, understanding the lithospheric structure beneath the CAP is helpful in guiding future mineral exploration (Downman et al., 2017; Duraiswami et al., 2014). For example, currently there is growing demand for REE and CAP is deemed to host a variety of such REE hence the need to further understand its structure and origin.

CHAPTER II

GEOLOGY OF THE CHILWA ALKALINE PROVINCE (CAP)

II.1. Tectonic setting

This work discusses the setting of the CAP within the framework of three tectonic elements. These are the Precambrian Southern Irumide belt and the Unango complex, the Mesozoic Karoo rift represented by the Shire graben, and the Cenozoic East African Rift System (EARS) represented by the Malawi rift (Figs. 1.1-1.4).

II.1.1. The Southern Irumide belt and the Unango complex

Different intrusive bodies of the CAP are found on the eastern side of the Southern Irumide belt and the western side of the Unango complex (Fig. 1.1). Both terranes are interpreted as Mesoproterozoic crust that was re-worked during the Neoproterozoic (Fritz et al., 2013). These Precambrian entities are bounded in the southeast by the NE-trending Lurio shear zone and to the southwest by the NW-trending Zambezi belt (Fig. 1.1). A recent study using regional magnetotelluric (MT) across the Southern Irumide belt in central Zambia and southwestern Malawi have shown that the center of the belt is underlain by a thick lithosphere (~250 km) typical of cratons and this has been termed the Niassa craton (Sarafian et al., 2018). The lithosphere of the Southern Irumide belt thins to the southeast reaching ~120 km close to the CAP (Sarafian et al., 2018).

The Precambrian rocks around the CAP are dominated in the southeast by what is referred to as the charnockitic suite which is made-up of banded proxene-granulites and gneisses and hypersthene granite and in the northwest by paragneisses, schists and granulites (Fig. 1.2). Narrow bands of schists, quartzites and marbles crop out within these two dominant lithologies (Fig. 1.2). These rocks are intruded by granitoids and migmatites (Fig. 2). These igneous activities include a phase of late Neoproterozoic alkaline magmatism (Bloomfield, 1968, 1970; Plat, 1986; Eby et al., 1998; Kroner et al., 2001; Ashwal et al., 2007, Broom-Fendley et al., 2016; 2017). This alkaline episode of magmatism is suggested to be associated with an ancient continental rift zone (Burke et al., 2003, Broom-Fendley et al., 2017). The regional Precambrian fabric in the southeast is characterized by the presence of NE-trending penetrative foliation (Fig. 1.2). However, this penetrative foliation assumes a more NW-trend to the northwest.

II.1.2. The Mesozoic Karoo rift

The earliest Karoo-related geological event around the CAP might be the emplacement of NE-trending Jurassic mafic dike swarm (Macdonald et al., 1983). These dike swarms can be clearly identified in the northeastern escarpment of the Shire graben through their appearance in the SRTM DEM as NE-trending topographic high and low lineaments (Fig. 1.4). Garson, (1960); Eby et al., (1998) and Dill, (2006) state that a great variety of sub-aerial volcanic, pyroclastic rocks as well as shallow sub-volcanic rocks formed in southern Malawi from Upper Jurassic through the lower Cretaceous and these are best exemplified by the exposures of the Lupata alkaline volcanic rocks to southwest of the CAP.

Dixey (1937) and Dixy et al. (1955) first recognized that the NW-trending Karoo rift (represented by the Shire graben to the southwest of the CAP; Fig. 1.4), although largely developed in Jurassic times, followed zones of Neoproterozoic crustal weakness represented by the Zambezi belt (Fig. 1.1) that developed during the Pan-African orogeny. Dixey (1937) and Dixy et al. (1955) explained that the Karoo rifting started with subsidence in the lower Shire and Zambezi valleys allowing for sediment accumulation in the resulting troughs. Further, Dixey (1937) and Dixey et al. (1955) speculated that a stage of intense fracturing and injection of doleritic dike swarms and sills and the outpouring of basaltic flows, which reached a thickness of 1200 m southern Malawi, followed sedimentation. Dixey (1937) and Dixey et al. (1955) further advanced the notion that after a period of erosion and towards the end of Karoo times, there was a renewed episode of sedimentation, which is marked in the Zambezi Valley by the deposition of arkosic sandstones, and was followed by the extrusion of thick rhyolite flows, which marked the end of Karoo activity. After a period of erosion after the end of Karoo times, which lasted some 30 Ma, sedimentation resumed with the deposition of conglomeratic sandstones and tuffs onto which 300 m of the Lupata lavas were erupted (Woolley, 1987)

II.1.3. The East African Rift System

The CAP is also found within the Shire horst, which represent the southeastern footwall of the Cenozoic Malawi rift, which is considered the southernmost segment of the Western Branch of the East African Rift System (EARS). The Shire highlands also represent the northeastern footwall of the Mesozoic Shire graben (Fig. 1.2). Some of the

CAP's bodies are clearly offset by the border normal faults of the Malawi rift (Figs. 1.2-1.4). However, some of the CAP intrusive bodies are also found on the floor of the Malawi Rift (Figs. 1.2-1.4). No significant sedimentation has accompanied rifting in southern Malawi rift. This is because both Precambrian crystalline rocks and some of CAP's intrusive bodies are found exposed on the rift floor (Fig. 1.2)

II.2. Geology, geochronology and geochemistry of the Chilwa Alkaline Province (CAP)

This region has been referred to as the CAP by Dixey et al. (1955); Garson (1965); Wooley and Garson (1970); and Vail (1989). The name Chilwa comes after the Lake Chilwa where a well-developed carbonatite ring complex is also located (Figs. 1.3 and 1.4; Vail, 1989). Geochemical analysis by Woolley and Jones (1987) established the CAP to constitute three igneous rock series: (1) syenite-quartz syenite-granite; (2) nepheline syenite-syenite; and (3) nephelinite-carbonatite-nepheline syenite. The syenite – quartz syenite – granite suite is represented by the Mulanje, Michesi, and Songwe-Mauze intrusions in the southeast and the Zomba-Malosa and Kapiri intrusion in the central part of the study area (Figs. 1.2 and 1.3). The nepheline syenite – syenite suite is represented by the Kangankkunde, Junguni, Chinduzi, Mongolowe, Chaone, and Chikala intrusions in the north as well as the Junguni intrusion further north of them. (Figs. 1.2 and 3). The Milange intrusion to the southeast of the Mulanje intrusion also belong to this suite. The nephelinite-carbonatite-nepheline syenite suite is represented by numerous carbonatite intrusions that are scattered throughout the CAP (Fig. 1.3). Other components of the CAP includes alkaline dike swarms following NE and NW-trending zones of

crustal weakness, small nephelinite, and phonolite plugs and small breccia vents (plat, 1986; Broom-Fendley et al., 2017).

The intrusions in the southeast forms the Mulanje Mountains as a number of overlapping circular intrusions reaching an elevation of ~3000m and has an average diameter of ~24 km (Fig. 1.4). The Zomba - Malosa Mountains is probably made-up of a single intrusion currently exposed with an elevation of over ~2000 m. (Fig. 1.4). The complex is surrounded on all but its northern sides by precipitous cliffs. In the west, it is truncated by the main NE-trending border normal fault of the Malawi rift (Figs. 1.2-1.4; Woolley and Jones, 1987). The Kapiri intrusion is found within the southeastern floor of the Malawi rift just to the west of the border normal fault (Figs. 1.2-1.4). This intrusion has poorly-defined surface expression in both the Landsat TM image and SRTM DEM compared to other intrusions (Figs. 1.3 and 1.4). The outcrops of the Kangankunde, Chinduzi, Mongolowe, Chaone and Chikala intrusions are defied by five intrusions aligned in an E-W direction extending from the Malawi rift floor to its eastern footwall (Figs. 1.3 and 1.4).

Several of the complexes have been isotopically dated using K-Ar method and have yielded mineral ages between 139 +/- 7 Ma (Tundulu carbonatite), 128 +/- 6 Ma (Mulanje syenite), 119 +/- 6 Ma (Chambe syenite) and 108 +/- 12 Ma (Zomba syenite) (Cahen et al.. 1984; Vail, 1989). Eby et al. (1998) found that the younging of individual CAP's intrusions is positively correlated with the silica enrichment. This led Eby et al. (1995; 1998) to categorize the CAP's intrusions into three age groups. These include basanite and nepheline synenite (138 Ma – 132 Ma), Nepheline syenite and syenite (129 Ma – 123 Ma), and syenite and granite (115 ma – 111 Ma). Eby et al. (1995; 1998)

attributed the positive correlation between the younging age of the CAP's intrusive bodies and silica enrichment to the increased crustal contamination of the magma with time. However, Eby et al. (1995; 1998) suggested that the CAP was sourced from a depleted mantle geochemical reservoir and it is geochemistry is suggestive of Oceanic Island Basalt (OIB).

CHAPTER III

DATA AND METHODS

This work used the Landsat TM (Fig. 1.3) with 30 m spatial resolution, SRTM DEM (Fig. 1.4), aeromagnetic data (Fig. 3.1) and Bouguer gravity anomalies from the WGM 2012 (Fig. 3.2) to study the lithospheric structure of the CAP. The Landsat TM 3-2-1 Red-Green-Blue (RGB) color combination and the hillshade SRTM DEM are primarily used to map the surface expression of the CAP as well as the brittle structures associated with the Shire graben and the Malawi rift to produce the modified map presented in Figure 1.2. Additionally, greyscale SRTM DEM is used as a background for draping geophysical images in order to correlate sub-surface features imaged by the geophysical data with the surface morphological expression of the CAP as in the case of Figure 3.1.

III.1. Aeromagnetic data enhancement

The Government of Malawi through the Ministry of Mining collected the aeromagnetic data in 2013 with NE-SW oriented flight lines. The spacing between the flight lines was 250 m, the spacing between the tie lines was 2.5 km while the average terrain clearance was 60 m. The data were processed in Geosoft Oasis Montaj. Firstly, the aeromagnetic data were reduced to pole to transform the magnetic data into vertical vector format (Baranov, 1957).

This transformation corrects the spatial location of the magnetic anomalies (Baranov 1957). Previous studies Katumwehe et al. (2015) have used the upward continuation filter to attenuate the near surface data, enhance deeper structures and this was used to produce a Total Magnetic Intensity (TMI) map (Fig. 3.2).

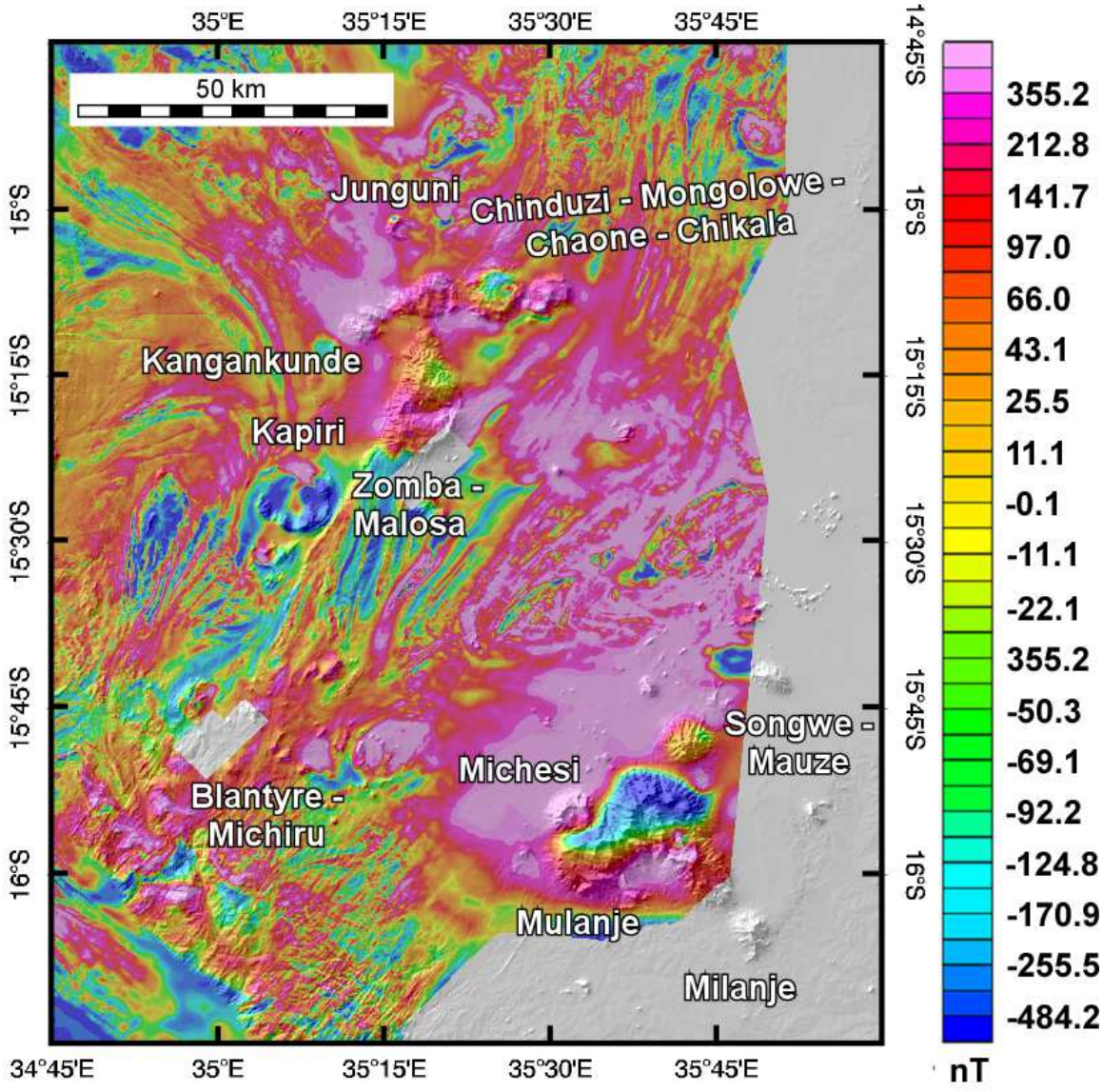

Figure 3.1: Total magnetic intensity (TMI) map of the Chilwa Alkaline Province (CAP) draped onto Shuttle Radar Topography Mission (SRTM) Digital Elevation Model (DEM).

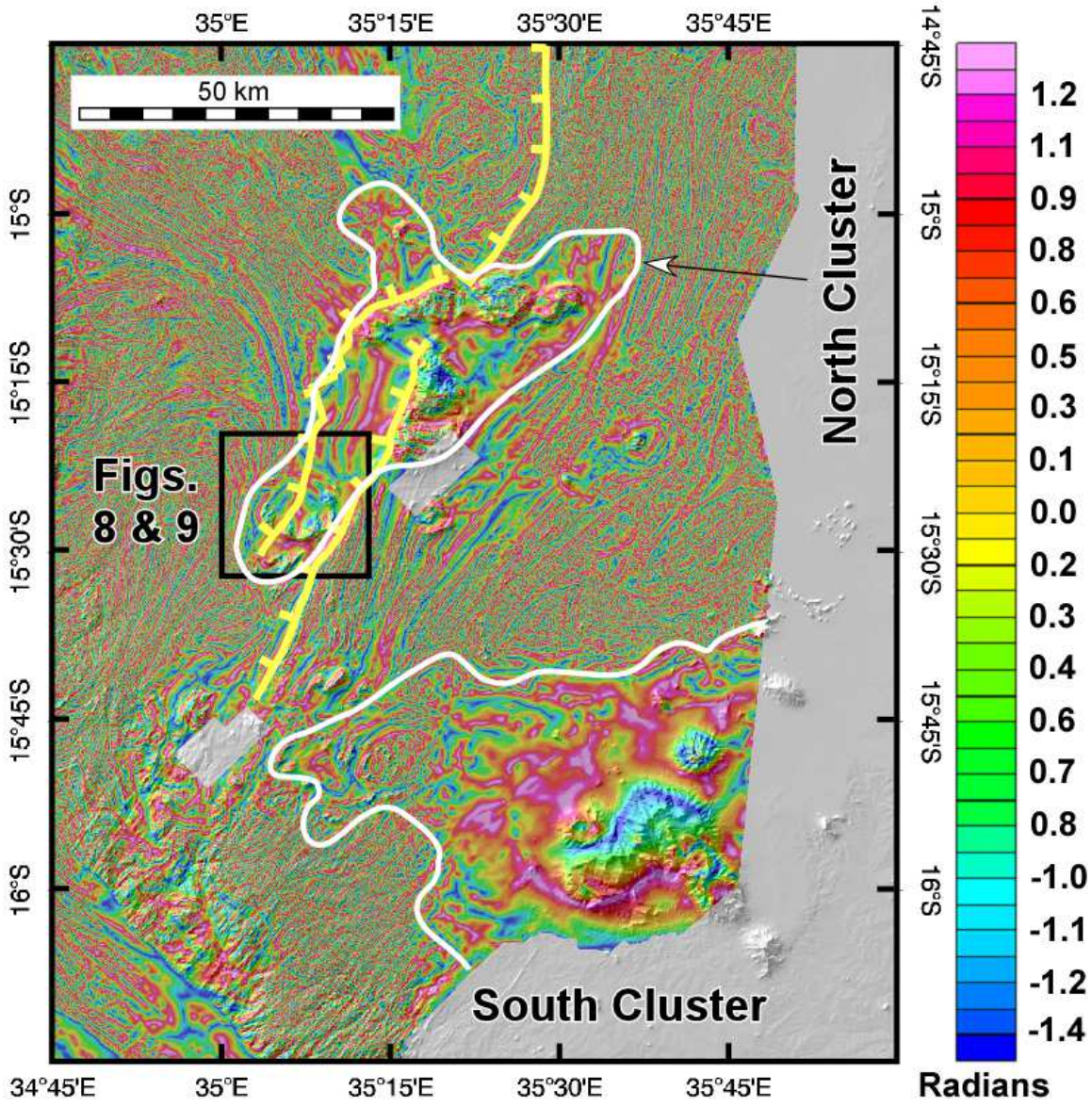

Figure 3.2: Tilt derivative mag of the Chilwa Alkaline Province (CAP) obtained from the total magnetic intensity (TMI) map of the aeromagnetic data. The white lines delineate the extent of the suggested north and south clusters of the CAP intrusive bodies. The yellow lines define the southeastern border normal faults of the Malawi rift. The ticks are on the hanging wall of the rift.

The tilt derivative filter(Miller and Singh,1994) was chosen to image the near surface geometry of the CAP as well as the surrounding Precambrian basement structures (Fig. 3.2). This is because the edge-detection filters have been proven successful in enhancing features such as Precambrian regional fabric (e.g. Katumwehe et al., 2016; Kolawole et al., 2017; 2018). The tilt derivative is the vertical derivative of the TMI divided by the total horizontal derivative of the TMI (e.g. Miller and Singh,1994; Katumwehe et al., 2016). For this, the tilt derivative filter was applied to the reduced to pole TMI data with the aim of enhancing the short wavelength magnetic anomalies associated with Precambrian basement structure as well as the contacts of different CAP's intrusive boundaries (Fig. 3.2).

III.2. The Voxi and magnetic susceptibility modeling of the aeromagnetic data

The Voxi Earth Modeling is an extension module in Geosoft Oasis Montaj that allows for 3D inversion of potential field geophysical data such as gravity and magnetics. The structural inversion uses Geosoft's GM-SYS 3D program with a voxel-based inversion (Pouliquen et. al., 2017). This allows for 3D imaging of the geometry of the density or magnetic anomaly sources and visualizing them by creating slices at various depths. The Voxi modeling utilizes a Cartesian Cut Cell (CCC) and an iterative reweighting inversion algorithm developed by Ingam et al. (2003). The filter uses a block of cells in which each cell is defined with a specific calculated density or susceptibility that is used to construct the 3D model for discrete bodies with unique density or magnetic anomaly ranges based on the Blakely theory. The 3D model solution defines the geometry of the individual magnetic anomaly sources. The only major problem of this

filter is that voxel inversions generally produce models, which have smoothed transitions between domains, whereas layered earth models need to have discrete transitions (Pouliquen et. at., 2017). This problem can be overcome through a series of constraints that can be set up during the voxel inversion to ensure that the layered nature of the physical properties distribution is honored. (Pouliquen et. al., 2017). The Inversions in this case can be completed as 'unconstrained' or 'constrained' using drill-hole information (e.g., magnetic susceptibility or density logs) or geological information. Gravity and magnetic data (ground or airborne data, total field or gradient measurements) can be inverted using different methods, and sets of constraints or regularizations (e.g., Barbosa and Pereira, 2013). In this work, we used the unconstrained modeling since we had no constraints.

Because of computational constraints that prevent development of 3D Voxi model for the entire CAP, this work selected the Kapiri intrusion (Fig. 3.2) to create a 3D Voxi model that exemplify other intrusions of the CAP. The Kapiri intrusion is selected because it is isolated and is not overlapping with other CAP's intrusion as well as that its surface expression is flat and not associated with high topography. Results of the 3D Voxi model are shown in Figure 3.3. In all, this method gives a better view of how the anomalous body is oriented in the subsurface (Fig. 3.3 and 3.4).

The magnetic susceptibility is a measure of the propensity of a material to become magnetized when placed in a magnetic field. It is also defined by $M = K H$, where M is the induced magnetization of the material and H is the inducing magnetic field strength. As both M and H are measured in amperes per meter, volumetric susceptibility K is a dimensionless quantity written as "SI", while mass susceptibility $X_{mass} = K/\rho$, where is ρ

is measured in $m^3 \cdot kg^{-1}$ in SI. In this work, we used the 3D Voxi model filtering to create a magnetic susceptibility model for the Kapiri intrusion (Fig. 6) to exemplify the magnetic susceptibility model of other CAP intrusions.

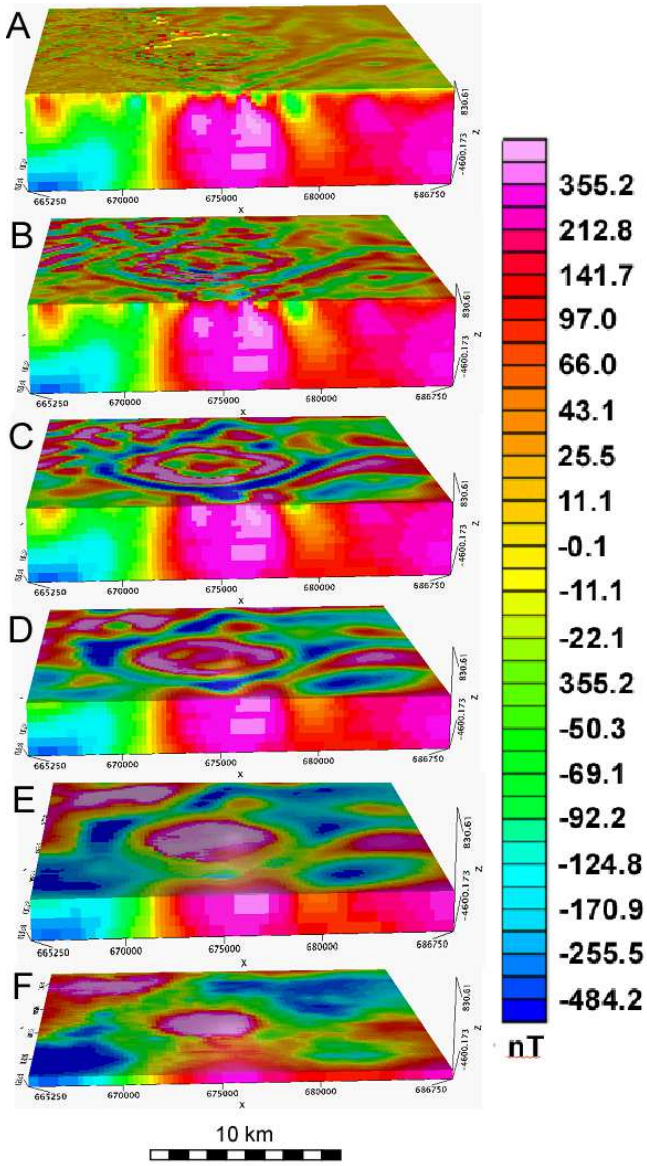

Figure 3.3: Three-dimensional (3D) Voxi model of the Kapiri intrusion of the Chilwa Alkaline Province (CAP) displayed as depth slices at 1 km above the surface (A), 0 km depth (B), 1 km depth (C), 3 km depth (D), 3 km depth (E), and 4 km depth (F). See Figure 6 for the location of the intrusion.

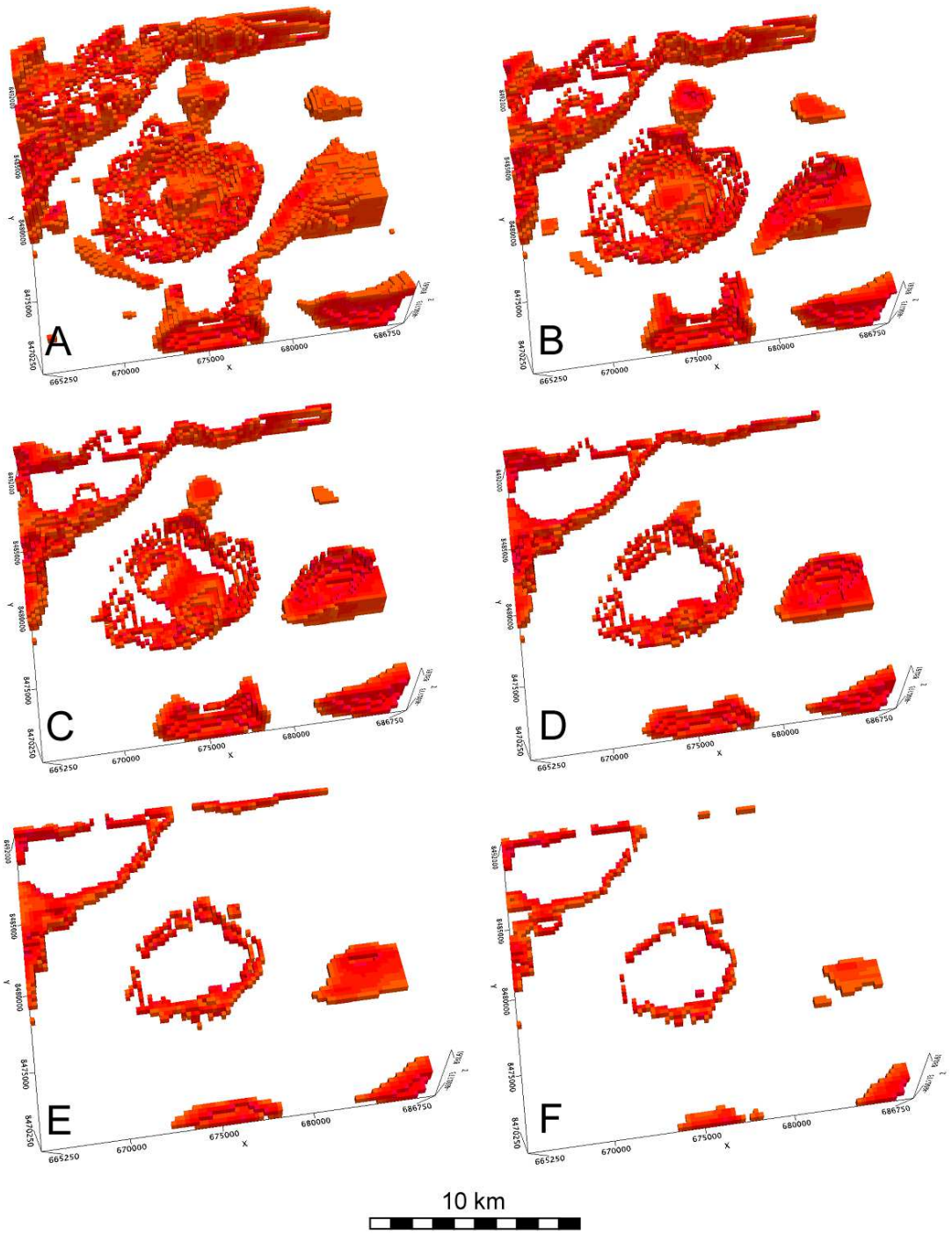

Figure 3.4: Three-dimensional (3D) magnetic susceptibility model of the Kapiri intrusion of the Chilwa Alkaline Province (CAP) displayed as depth slices at 0 km (A), 1 km (B), 2 km (C), 3 km (D), 4 km (E), and greater than 5 km (F). See Figure 6 for the location of the intrusion.

Sources of magnetic susceptibility and their anisotropy provide the most fundamental data for the interpretation of magnetic surveying (e.g. Borradaile, 1987). Careful spatial analysis may reveal emplacement kinematics or locate the magma source (e.g., Borradaile, 1987). In this work, we used the 3D Voxi model filtering to create a magnetic susceptibility model for the Kapiri intrusion (Fig. 3.3).

III.3. Satellite Gravity Data (World Gravity Model 2012 (WGM2012)

The gravity data used in this study were obtained from the WGM 2012 (Balmino et al., 2012; Bonvalot et al., 2012). The spatial resolution of the WGM 2012 is ~9 km. Taking into account the real topography of the Earth, which is in reference to a spherical prism, the global Bouguer gravity anomalies were computed based on the spherical terrain correction (Balmino et al., 2012). The Earth's Topography derived Gravity model (ETOPG1) was subtracted from the Earth Gravity Model 2008 (EGM 2008) in this method. The EGM2008 comprises of land, airborne, and marine surveys, which are surface gravity measurements. It also comprises of measurements from satellite altimetry and satellite gravimetry of the Gravity Recovery and Climate Experiment (GRACE) mission (Bonvalot et al., 2012). The ETOPG1 was obtained from the spherical harmonic analysis of the heights of the Earth's topography-bathymetry components from the 1°X1° spatial resolution Global Topographic 30 arc second (GTOPO30) database. The Bouguer gravity anomaly map of the WGM 2012 after 2 km upward continuation covering the CAP and its surroundings is shown in Figure 3.5.

III.4. Upward Continuation of the Bouguer Gravity Anomalies

Potential fields known at a set of points can be expressed at neighboring higher or lower spatial locations in a source free region using the continuation integral that results from one of Green's theorems (Blakely, 1996, Ravat, 2007; Hemanta et al., 2007). The main idea in this concept is to adjust altitude of observations to a datum as an aid to the interpretation of a survey (Ravat, 2007; Hemanta et al., 2007). By upward continuation of the gravity field, short-wavelength gravity anomalies are reduced, and continuing the field downwards, increases the horizontal resolution of the gravity anomalies and their sources.

The effect of upward or downward continuation process on the gravity fields can be understood by examining the continuation operator in the wavenumber domain. The operator has the form $\mathbf{e}^{\pm|\mathbf{k}|z}|$, where $|\mathbf{k}|$ is the wavenumber $\mathbf{(|k|)} = \mathbf{2\pi\lambda}$ where $\boldsymbol{\lambda}$ is the full wavelength and z is the continuation level (e.g. Ravat, 2007). The negative sign in the exponent indicates upward continuation, which is away from the sources of the field, and the positive sign implies the downward continuation, which is towards the sources of the field (Ravat, 2007). Both operations are susceptible to errors if the data for example, have measurement errors. Then the nature of downward or upward continuation operator, which amplifies primarily either the shortwave or longwave components of the data, can severely distort the downward and upward continued result (Ravat, 2007).

Furthermore**,** the upward continuation involves mathematically continuing the gravity field from one elevation to a higher elevation, in order to remove the effect of near surface and shorter wavelength gravity anomalies (Jacobsen, 1984; Zeng et al., 2007). Jacobsen (1984) used upward continuation of the gravity field to a specific height

(Z) where the depth of the sources is at or below half the continuation distance. The sum of gravity anomalies due to lateral variations in density within different lithological units in the near-surface and deeper within the Earth give the observed Bouguer gravity anomaly. It is therefore essential to identify contributions due to variations in density occurring at different depths (Gómez-Ortiz et al., 2011). In this case, high-frequency components of the observed Bouguer gravity anomalies are usually attributed to shallow depths, and low-frequency components are attributed to deeper depths. This is because the deeper the gravity source, the weaker the signal (low frequency) as the energy due to the force of attraction between the gravity source and the sensor is spread over a wider spectrum.

In this work, the observed Bouguer gravity anomalies of the WGM 2012 covering the CAP and its surroundings were upward continued to 2 km in order to attenuate the unwanted high-frequency anomalies due to near-surface (<2 km) features, while accentuating deep-source low-frequency anomalies (Fig. 3.5). Farther, in order to remove the influence of more high frequency anomalies, and estimate the depth extent of the intrusive bodies of the CAP we applied an upward continuation filter to the Bouguer gravity anomalies of the WGM 2012 by 4 km, 6 km, 8 km, 10 km, 12km, and 15 km (Fig. 3A-F).

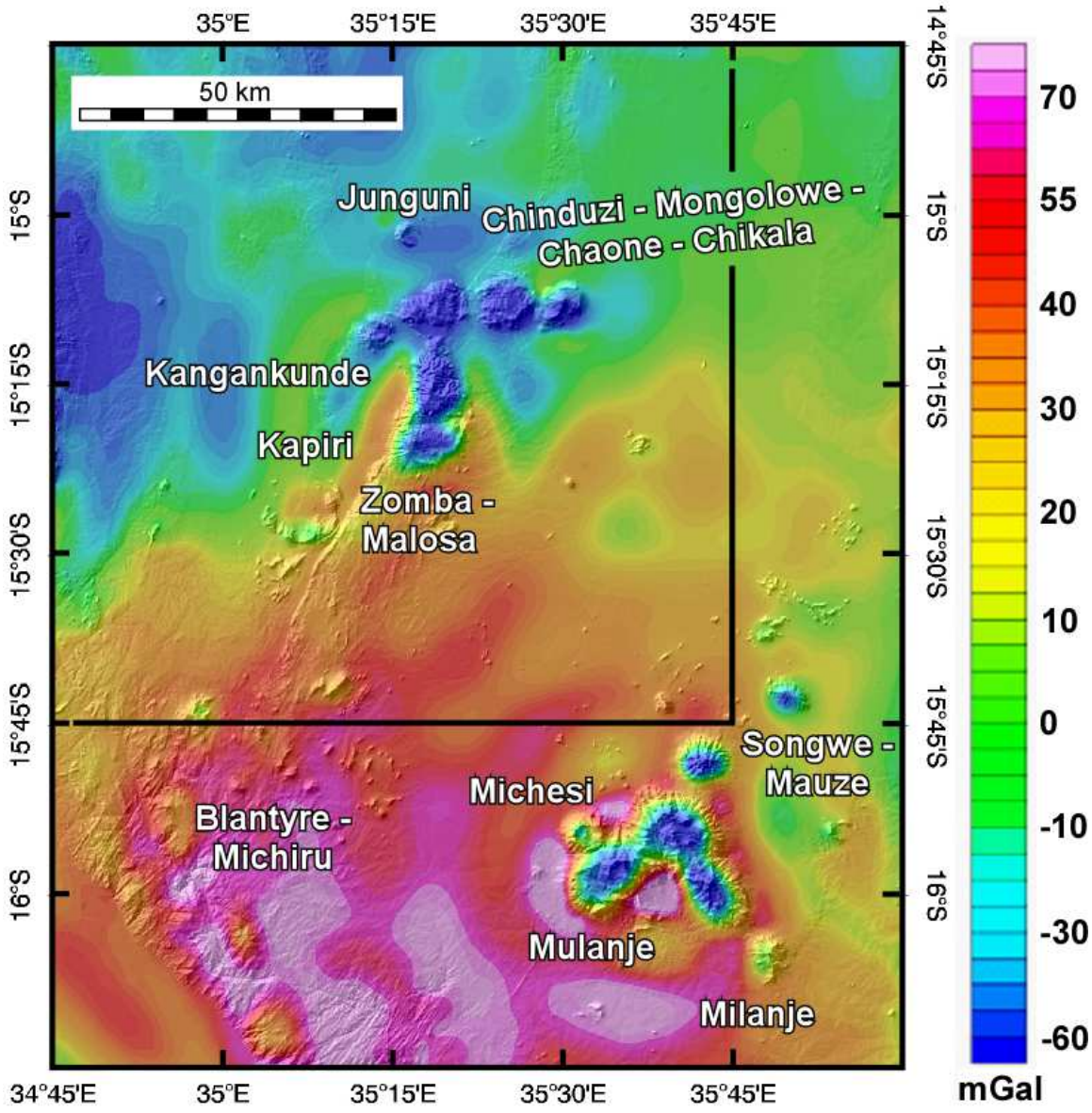

Figure 3.5: Bouguer gravity anomaly map of the Chilwa Alkaline Province (CAP) extracted from the World Gravity Model 2012 (WGM 2012). The Bouguer gravity anomaly map is draped onto Shuttle Radar Topography Mission (SRTM) Digital Elevation Model (DEM). These data are used for estimating the depth to Moho and the lithosphere-asthenosphere boundary (LAB) beneath the CAP and its surroundings using the two-dimensional (2D) radially averaged power spectrum analysis. The black box represents the location of the ~110 km x 110 km sub-region used for the generation of the spectral curve shown in Figure 11.

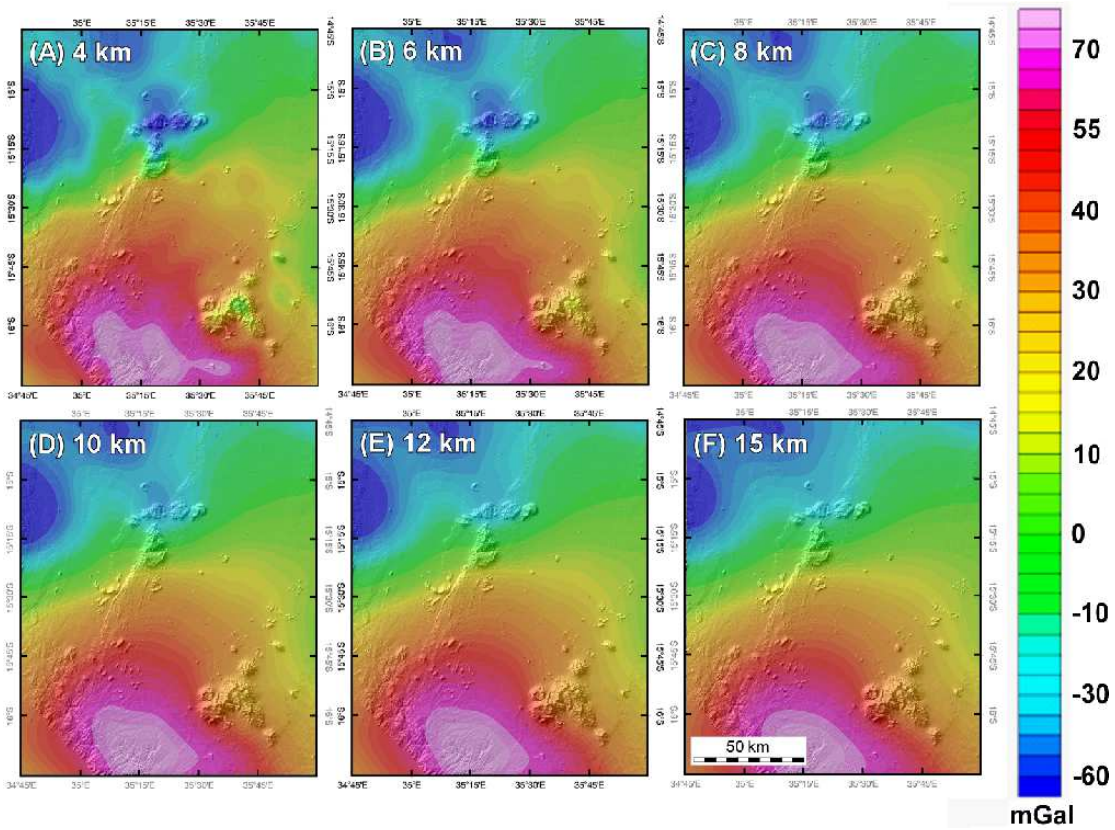

Figure 3.6: Upward-continued Bouguer gravity anomalies of the World Gravity Map 2012 (WGM 2012) of the Chilwa Alkaline Province (CAP) at 4 km (A), 6 km (B), 8 km (C), 10 km (D), 12 km (E), 15 km (F).

III.5. Two-dimensional (2D) radially average power spectral analysis

This study used the spectrum analysis that was developed by Tselentis et al., (1988) to estimate the depth to Moho and the LAB beneath the CAP and its surroundings using the Bouguer gravity anomalies of the WGM 2012. Russo and Speed (1994) stated that the power spectrum is the description of how the power of the gravity response is distributed over different frequencies (or wavenumbers). In this study, the power spectrum was used on the 2 km upward continued Bouguer gravity anomalies of the WGM 2012 using window sizes of 110 km X 110 km. These sub-windows were overlapped by 75% on all sides in order to minimize the Gibbs phenomena and to increase data resolution. The 75% overlap

of the sub-windows is ideal for realizing an increased spatial resolution, hence allowing detailed average depths of the Moho and the LAB. The Bouguer gravity anomalies from the WGM 2012 for each sub-window were transformed from the space domain to the frequency domain by means of a Fast Fourier Transform (FFT) before calculating the power spectrum. This transformation engenders the Gibbs phenomena in which the boundaries of the windows behave as a jump discontinuity (edge effect).

The natural logarithm of the power spectrum (Ln (power spectrum) is plotted against the wavenumber (k) to produce the spectral curve for each sub-window. An example of the spectral curve of a sub-window covering 110 km X 110 km is presented in Figure 11. The location of the sub-window is shown in Figure 9. The spectral curves have three linear segments and the breaks in their slopes represent density discontinuities at different depth (Fairhead and Okereke, 1987; Tselentis et al., 1988; Gómez-Ortiz et al., 2005; 2011). Each of the linear segments is associated with a range of wavenumbers and provides an indication of their average depth (Gómez-Ortiz et al., 2005; 2011). The lowest wavenumbers segment of the spectral curve represents the sharp density contrast across the LAB, while the intermediate wavenumbers portion of the spectral curve represents the sharp density contrast across the Moho. The highest wavenumbers segment of the spectral curve possibly relates to shallow boundaries within the crust but can also be noise that is contained in the data.

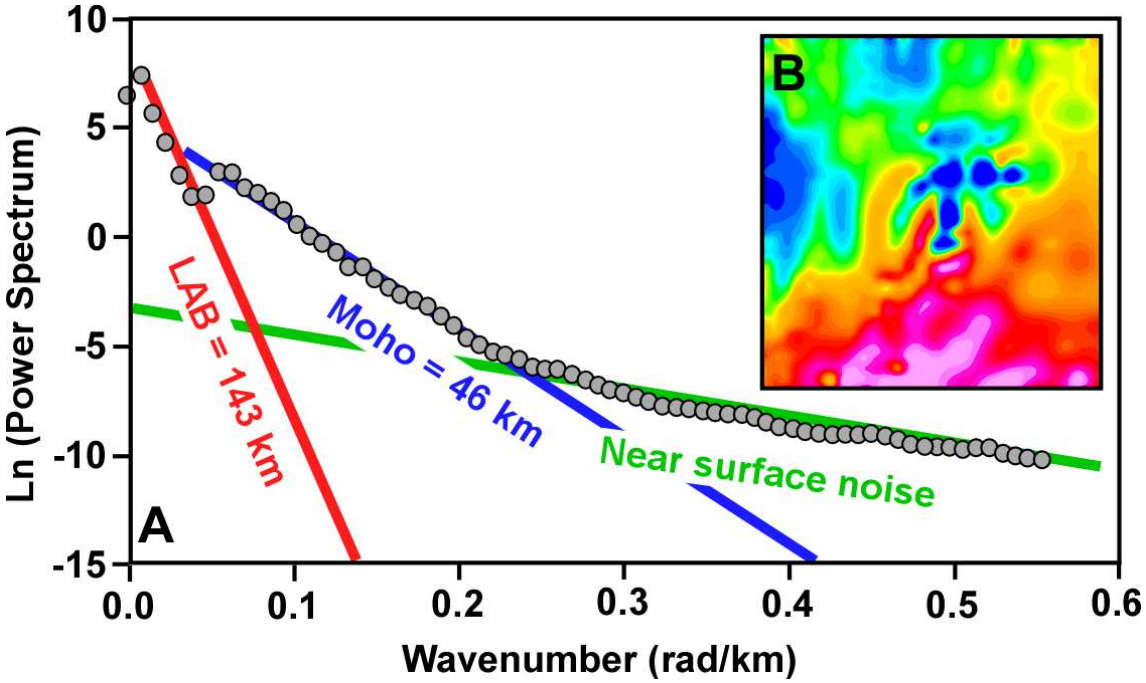

Figure 3.7: (A) An example of the two-dimensional (2D) radially-averaged power spectral curve used for the estimation of the depth to Moho and the lithosphere-asthenosphere boundary (LAB) from the Bouguer gravity anomalies of the World Gravity model 2012 (WGM 2012). (B) The Bougure gravity anomaly map of the (~110 km x 110 km sub-region used to generate the spectral curve. See Figure 9 for the location of the sub-region.

CHAPTER IV

RESULTS

IV.1. Magnetic fabric of the Chilwa Alkaline Province (CAP) and its surroundings from the Total Magnetic Intensity (TMI) and the tilt derivative map of the aeromagnetic data.

The TMI and the tilt derivative maps show a number of features related to the CAP, the Precambrian crystalline basement, the Shire graben, and the Malawi rift (Figs. 3.1 and 3.2). (1) Generally, the Precambrian crystalline basement is shown with dominantly short wavelength magnetic lineation that has a NE-trend within the Shire highlands in the southeastern part of the study area. This magnetic lineation becomes NW-trending in the northwestern part of the study area within the Precambrian crystalline basement that is exposed in the floor of the Malawi rift. This short wavelength magnetic lineation represents the regional fabric of the Precambrian crystalline basement. The change in the trend of the magnetic fabric generally coincides with the southeastern border normal fault of the Malawi rift (Fig. 3.2). It also coincides with the geological contact between the charnockitic suite in the southeast and the paragneisses, schists and granulites to the northeast (Compare Figs. 1.2 and 3.2). (2) In the southwestern part of the study area, the NE-trending magnetic lineation representing the Precambrian crystalline basement fabric sharply terminates against a broader wavelength NW-trending magnetic lineation associated with the Shire graben (Fig. 3.2) and this magnetic anomaly possibly represents the graben sediment infill. (3) The TMI map shows some of the CAP intrusive bodies characterized by low magnetic anomalies compared to the surrounding

Precambrian crystalline basement and this is especially true for the central part of the Mulanje Mountains and the Kapiri intrusion (Fig. 3.1). The TMI map also shows portions of the Shire graben characterized by low magnetic anomalies too. (4) The tilt derivative map shows that the CAP intrusive bodies as possibly belonging to two broad cluster. The southern cluster includes the Mulanje, the Songwe – Mauze, the Michese, and possibly three additional igneous ring complexes that have not been identified before (Fig. 3.2). The northern cluster includes the Kapiri, the Zomba-Malosa, the Chinduzi, Mongolowe, Chaone, Chikala, and the Junguni cluster. The tilt derivative map also revealed that the Junguni intrusion is much larger than what its surface expression is indicating (Compare Figs. 1.4 and 3.2).

IV.2 The geometry of selected Chilwa Alkaline Province (CAP) intrusions from the three-dimensional (3D) Voxi modeling and magnetic susceptibility analysis of the aeromagnetic data

The 3D Voxi model of the Kapiri intrusion is displayed by six depth slices at 1 km above the surface, at 0 km depth, and at 1 to 4 km depth at 1 km interval (Fig. 3.3). At all depth, the Karipi intrusion is depicted by circular high magnetic anomalies. This might be due to the presence of higher concentration of magnetic minerals within the intrusion compared to the surrounding Precambrian crystalline basement. This model also shows that the magnetic anomalies depicting the Kapiri intrusion are in the form of narrow concentric features at upper levels (1 km above the surface and at 0 depth) and these thinner anomalies become wider by merging into each other at shallow depth (1 km and 2 km depth) until they form a single circular magnetic anomaly at deeper depth (3 km

and 4 km depth). This geometry is interpreted as a system of concentric fractures developed during the caldera collapse and these where filled with magma forming ring dikes. The concentric fracture system filled with magma becomes less dense at deeper depth until it merges with sub-horizontal sheet intrusions.

The 3D magnetic susceptibility model of the Kapiri intrusion is represented by six depth slices at 0 km to 4 km at interval of km and then greater than 5 km (Fig. 3.4). Different magnetic susceptibility values were considered with values ranging between 0.001 and 0.27 SI to effectively separate the geometry of the Kapiri intrusion form the surrounding Precambrian crystalline basement. At depth of 0 km to 2 km, the magnetic susceptibility model shows the Kapiri intrusion as a single circular feature (Fig. 3.4A-C). However, at depth of 3 km to 5 km and greater the model shows the intrusion as a ring feature (Fig. 3.4D-F).

IV.3. Upward continuation of gravity data

The upward continuation images of the Bouguer gravity anomalies of the WGM 2012 of the CAP and its surrounding show sharp contrast between the northwestern and southern part of the study area (Fig. 3.6). The northwestern part is characterized by semi-circular gravity low anomaly (reaching -60 mGal) within the Malawi rift, which seems to persist to a depth of ~7.5 km (half of the upward continuation to 15 km) (Fig. 3.6F). The southern part is characterized by an elliptical gravity high anomaly (reaching 70 mGal) extending on the northeastern footwall of the Shire graben, and equally this anomaly persists to a depth of 7.5 km (Fig. 3.6F). This difference in gravity anomalies cannot be explained as due to the presence of graben sediment fill within the Malawi rift. This is

because the Precambrian crystalline basement is exposed in the floor of the rift (Fig. 1.2). Rather, as the geological map in Figure 1,2 shows, the Precambrian crystalline basement rocks exposed within the Malawi rift floor are less dense and constitute paragneisses, schist and granulites. Differently, within the Shire highlands the Precambrian crystalline basement rocks are made-up of denser lithologies including the charnockitic suite, which is made-up of banded pyroxene-granulites, gneisses and hypersthene-granite (Fig. 1.2).

The cluster of the Junguni - Chinduzi – Mongolowe – Chaone – Chikala – Kangankunde - Zomba – Malosa cluster crops out on the southeastern side and within the Malawi rift where the regional gravity low anomaly is imaged (Fig. 3.6). The upward continuation images of the Bouguer gravity anomalies of the WGM 2012 shows this cluster is characterized by a localized and relatively lower gravity anomaly (compared to the broader gravity low anomaly) and that persists to a depth of ~6 km (Fig. 3.6E). Also, the upward continuation images show that the Mulanje – Michesi – Songwe – Mauze – Milanje cluster is characterized by a relatively lower gravity anomaly that disappears at a depth of ~ 4 km (Fig. 3.6C). It is possible that the gravity anomalies associated with the two clusters represent the deeper structures of the CAP now preserved as a crystallized magma chamber or broad batholiths.

IV.4. The Moho and Lithosphere-Asthenosphere Boundary (LAB) depth from the two-dimensional (2D) radially-averaged power spectral analysis of the Bouguer gravity anomalies of the World Gravity Model 2012 (WGM 2012)

The Moho depth estimates obtained from the two-dimensional (2D) radially-averaged power spectral analysis of the Bouguer gravity anomalies of the World Gravity

Model 2012 (WGM 2012) beneath the CAP and its surroundings range between ~38 and ~45 km (Figure 4.1). In here, we observe that there is no consistent pattern of crustal thinning following the surface expression of the Shire graben or the Malawi rift. Generally, it is found that the thickest crust reaching ~45 km is found within the Shire horst beneath the CAP (Fig. 4.1). This is consistent with results of spectral analysis of the Bouguer gravity anomalies of the WGM 2012 that was conducted for the entire Malawi rift (Njinju et al., in review).

No Moho depth estimates are available for the CAP and its surroundings from receiver function analysis of passive seismic data. However, recent studies from the Congo craton (Goussi Ngalamo et al., 2017) and the Southern Main Ethiopian Rift (Emishaw et al., 2017) have quantitatively shown the consistency of Moho depth estimates results obtained from the spectral analysis of the Bouguer gravity anomalies of the WGM 2012 and those obtained from the receiver function analysis of the passive seismic data. We also note that

Our LAB depth results beneath the CAP and its surroundings based on the spectral analysis of the Bouguer gravity anomalies of the WGM 2012, range between ~110 km and ~165 km (Fig. 4.1). It is noted that the Shire graben and the Malawi rift are underlain by relatively thicker lithosphere (the LAB depth is ~160 km) compared to the southeastern part of the Shire horst beneath the Mulanje Mountains (the LAB depth is ~110 km) (Fig. 4.2). This is consistent with results of spectral analysis of the Bouguer gravity anomalies of the WGM 2012 that was conducted for the entire Malawi rift where the LAB is imaged at depth as deep as ~205 km in regions away from the CAP and its surroundings (Njinju et al., in review).

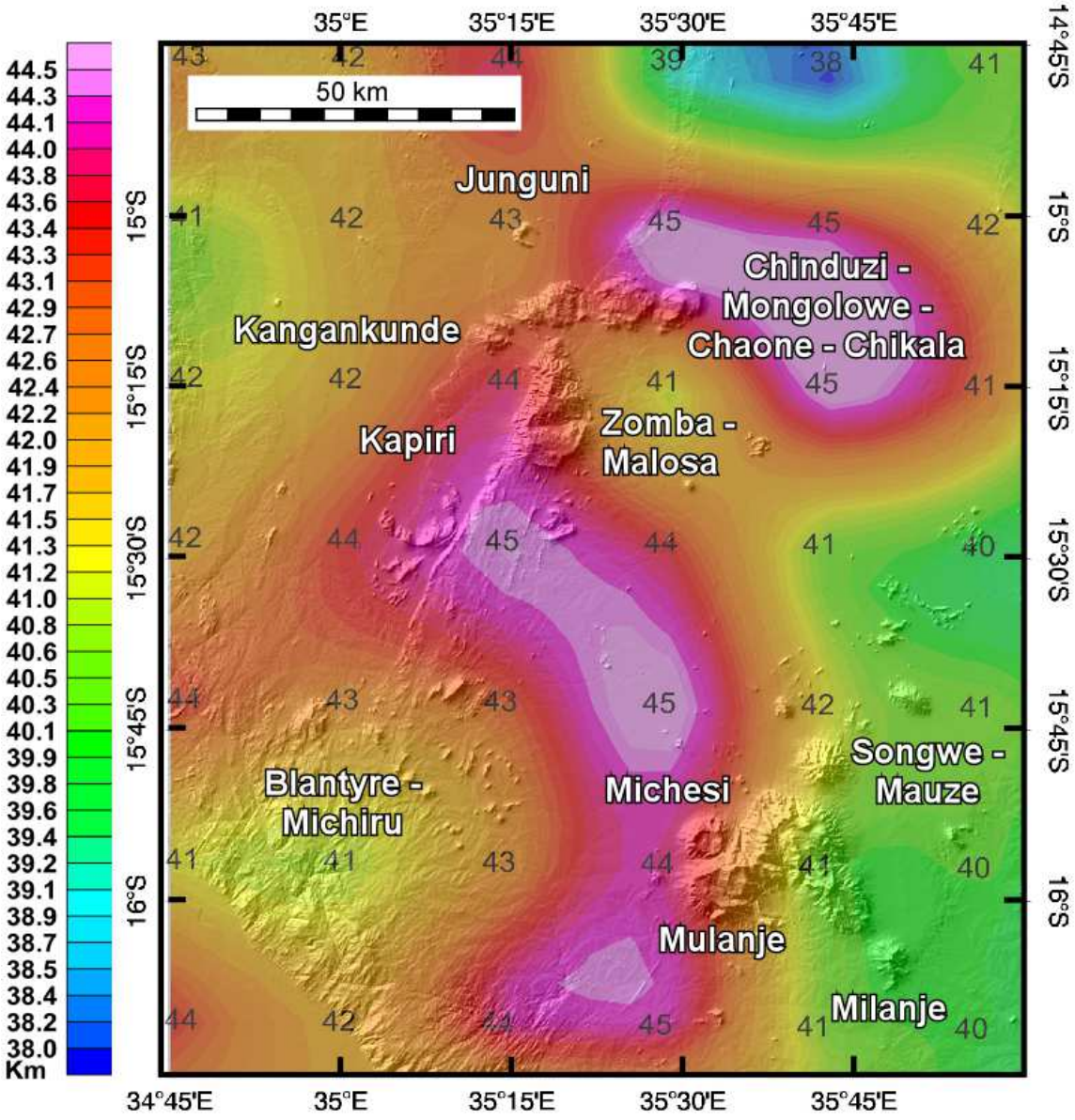

Figure 4.1: Crustal thickness map of the Chilwa Alkaline Province (CAP) obtained from the two-dimensional (2D) radially-averaged power spectral analysis of the Bouguer gravity anomaly of the World Gravity Model 2012 (WGM 2012).

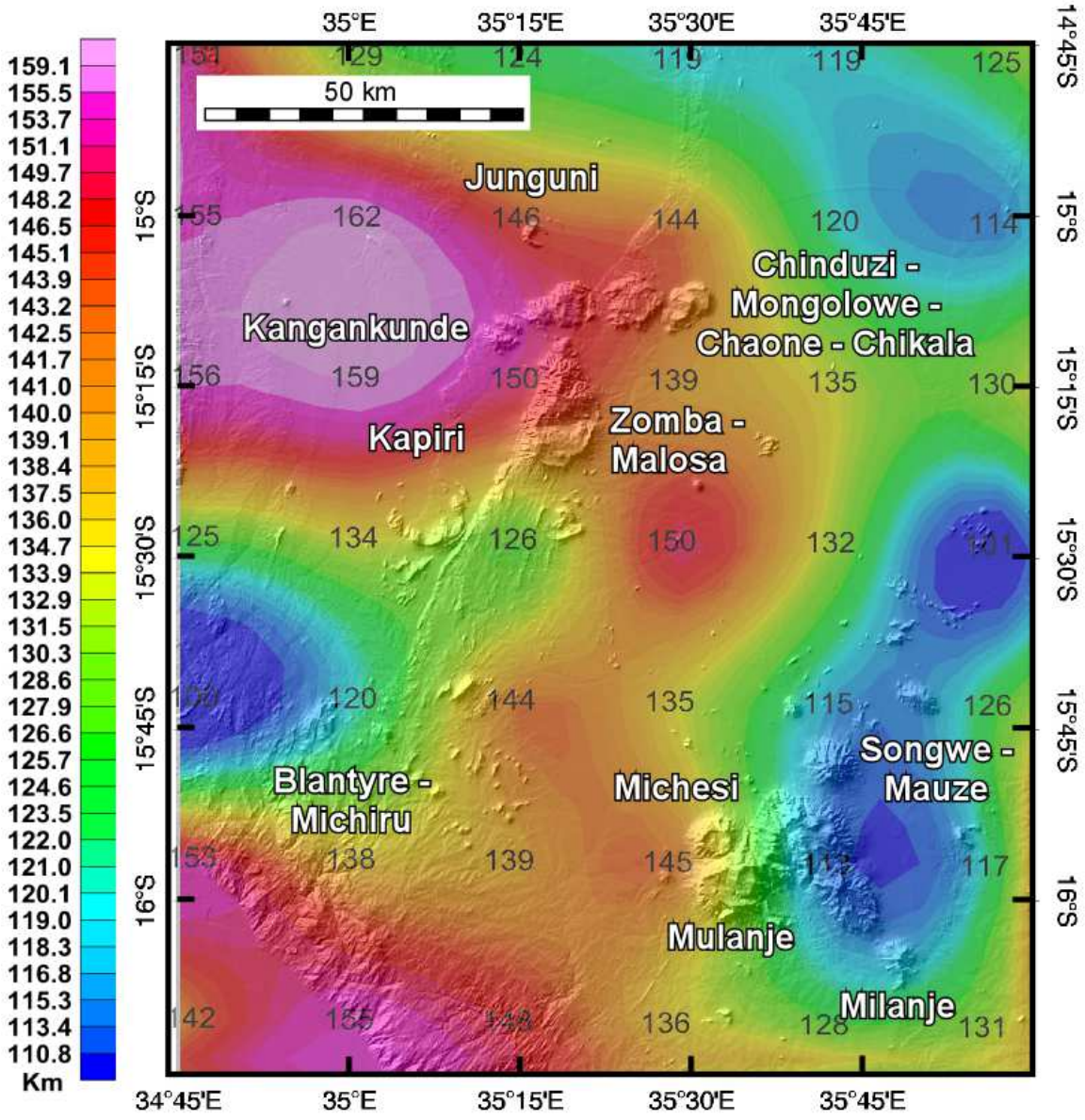

Figure 4.2: Lithospheric thickness map of the Chilwa Alkaline Province (CAP) obtained from the two-dimensional (2D) radially-averaged power spectral analysis of the Bouguer gravity anomaly of the World Gravity Model 2012 (WGM 2012).

CHAPTER V

DISCUSSION

V.1 The geometry of the magmatic plumbing system of the Chilwa Alkaline Province (CAP)

One of the findings of this study (from the tilt derivative of the aeromagnetic data and the upward continuation of the Buouguer gravity anomalies of the WGM 2012) is the presence of two distinct clusters (northern and southern) of the intrusions constituting the CAP (Fig. 3.2). This study proposes that the magmatic sources of the intrusions constituting the CAP might have been two separate magma chambers at depth between ~4 km and ~6 km since these two do not coalesce to form one igneous intrusion at depth. This study also suggests that the southern cluster of the CAP has more intrusions than what appears on the surface and these were emplaced at shallower depth than those in the northern cluster (Fig. 3.2).

As exemplified by the Kapiri and the Michesi intrusions, results of this study (from 3D Voxi modeling and magnetic susceptibility analysis) show that the ring complexes of the CAP are highly magnetized and they were emplaced at different levels, which can be attributed to multiple episodes of magmatic eruptions within the region. Magnetic susceptibility of some of the ring complexes show mostly an upward movement of the magma related fluids with the region.

V.2. The origin of the thick crust beneath the Chilwa Alkaline Province (CAP).

The presence of thick crust (~40 km – ~45 km) beneath the CAP and its surroundings can be attributed to two geological events. First, it is possible that the thicker crust beneath the CAP was due to Neoproterozoic collisional events. It is likely that crustal thickening during the Neoproterozoic is associated with crustal shortening across the Lurio shear zone, which represent the boundary between the Southern Irumide belt and the Unango complex (Fig.1.1) in the northwest on the one hand, and the Nampula complex to the southeast on the other hand (Fig.1.1). For example, Fritz et al. (2013) used metamorphic pressure – temperature estimates from the Ocua complex granulites that decorate the Lurio shear zone to suggest that the formation of the belt was associated with significant crustal thickening possibly producing a crust as thick as 50 km. It is also possible that the thicker crust beneath the CAP was formed due to mafic magmatic under-plating (Thybo and Artemieva, 2013). It could be argued that these mafic magmatic under-plating events occurred during the Neogene in association with the development of the Malawi rift. However, no Neogene volcanic activities is reported in the vicinity of the CAP. Hence, it is likely that the mafic magmatic under-plating event occurred during the Cretaceous in association with the CAP. Hence, this work concludes that the thick crust beneath the CAP and its surroundings was due to a combination of the Neoproterozoic collisional events as well as the Cretaceous mafic magmatic under-plating event. This work propose that the mafic magmatic under-plating resulted in partial melting of the lower crust that progressively changed the magma feeding the CAP

to be more felsic with time as has been suggested from petrographic, geochemical and geochronological studies (Eby et al., 1995; 1998).

V. 3 The origin of the thin sub-continental lithospheric mantle (SCLM) beneath the Chilwa Alkaline Province (CAP)

Results of this study show a general thinning of the LAB beneath the CAP and its surroundings. It is noted that thinning of the LAB is highest in the southeastern side of the Shire horst beneath the southeastern side of the Mulanje Mountains (Fig. 4.2). This is where the Neoproterozoic Lurio shear zone is exposed representing the boundary between the Southern Irumide belt and the Unango complex in the northwest on the one hand and the Nampula complex to southeast on the other hand (Fig. 1.1). This boundary is not considered to be a Precambrian suture zone (Viola et al., 2008). However, Fritz et al. (2013) considered it to be "a site of significant and prolonged strain accommodation". Hence, it is possible that this zone facilitated lithospheric thinning during a NW-SE directed extension during the Mesozoic Karoo rifting event. NW-SE extension during the Karoo rifting event is plausible because: (1) a number of Karoo rifts are oriented NE-SE. These include, north of the CAP, the Luangwa rift and the Maniamba trough (Fig. 1.1). (2) The presence of NE-trending Karoo dike swarm in the southwestern part of the study area within the footwall of the Shire graben (Fig. 1.4).

This work proposes that thinning of the SCLM beneath the CAP and its surroundings allowed for the ascendance of the asthenosphere (to a depth of ~110 km)

and this resulted in decompression melting. As noted by Rychert and Shearer (2009) and Eaton et al. (2009), the LAB is a significant mechanical boundary that separated the SCLM that has a quasi-rigid behavior from the asthenosphere which behaves in a more viscous manner. It is also noted that the LAB lies close to the solidus of the asthenosphere. Hence, thinning of the SCLM during extension (Crough, 1983; Morgan, 1984; Neugebauer et al., 1987) will result in adiabatic advection of the asthenosphere (Keen et al., 1994) to cross its solidus line, hence melt by decompression.

V.4. Lithospheric-scale model for the Chilwa Alkaline Province (CAP)

This study proposes a lithospheric-scale model for the CAP that include (Fig. 5.1): (1) Thickening of the crust beneath the CAP during the Neoproterozoic due to shortening across the Lurio shear zone possibly due to convergence between the Southern Irumide belt and the Unango complex in the northwest on the one hand and the Nampula complex to the southeast on the other hand. (2) Thinning of the lithosphere beneath the CAP during the Cretaceous due to NW-SE extension associated with the Karoo rifting event. This lithospheric thinning might have been localized by the presence of the Neoproterozoic Lurio shear zone. (3) Thinning of the lithosphere resulted in the ascendance of the asthenosphere to as much as ~110 km deep, hence resulted in its decompression melting to produce magma with mantle geochemical signature. (4) Portion of the ascending mantle melt was accreted at the base of the crust as mafic magmatic under-plating resulting in additional thickening of the crust.

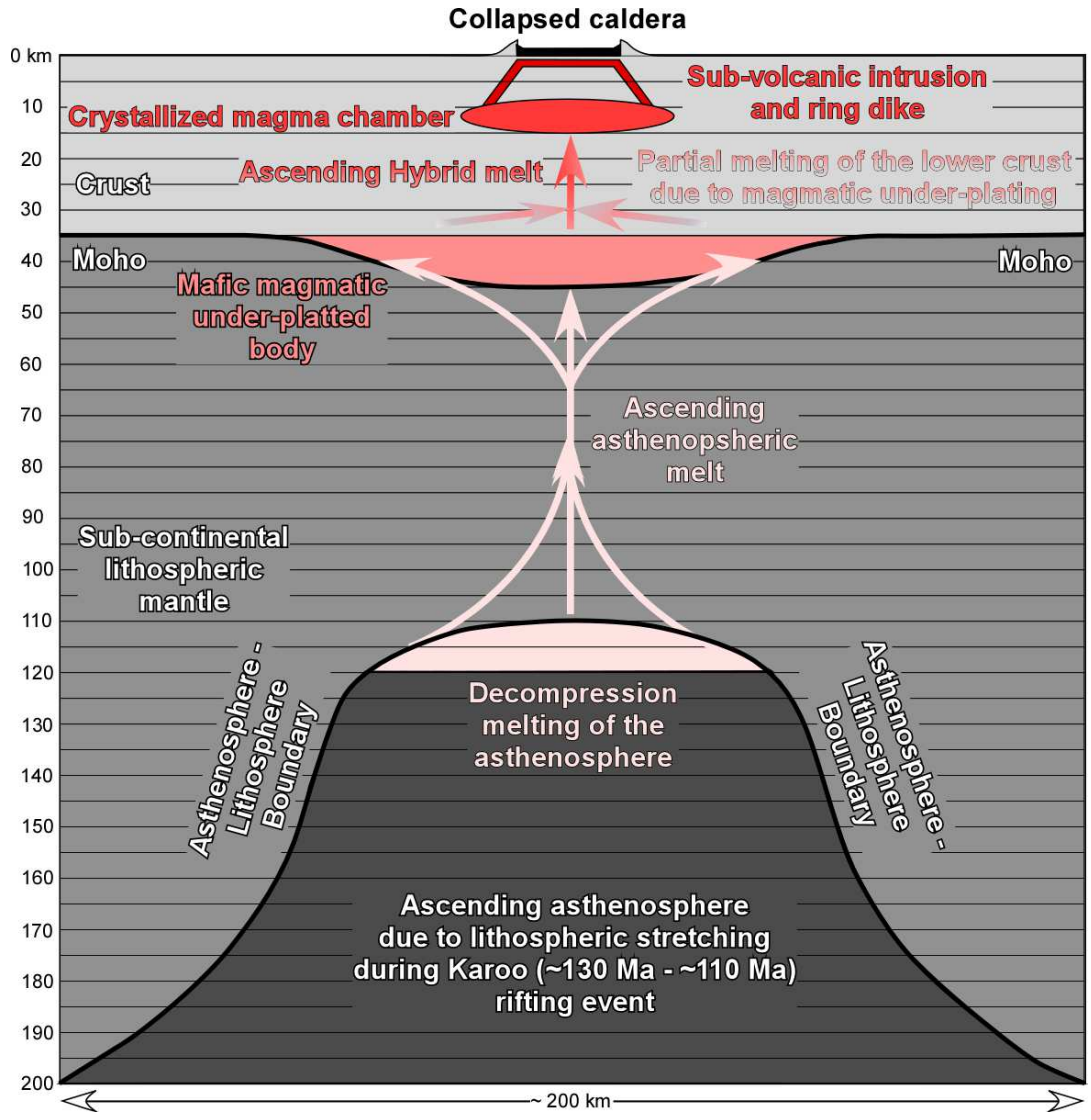

Figure 5.1: Conceptual model showing the Chilwa Alkaline Province (CAP) as being formed due to: (1) Decompression melting of the asthenosphere because of lithospheric stretching during Karoo (130 Ma – 110 Ma) rifting event. (2) Ascendance of the asthenospheric melt to the base to the base of the crust where it was partially accreted to for a mafic magmatic under-platted body. (3) Partial melting of the lower crust due to heating from the mafic magmatic under-platted body. (4) Mixing of the lower crust melt with the remainder of the ascending asthenospheric melt. (5) Formation of a shallow (top is ~8 km) magma chamber that was fed from the ascending hybrid melt. (6) Formation of individual ring complexes as collapsed caldera underlain with sub-volcanic intrusions and ring dikes.

(5) The mafic magmatic under-plating provided enough heat to partially melt the lower crust, hence produced melt with distinct geochemical crustal signature, which mixed with the portion of the mantle melt, which did not accrete at the base of the crust and ascended through the crust. (6) The mixed magma ascended to shallower levels to feed ~4 km to ~6 km deep magma chambers, which were later crystallized to form broad batholiths. (7) The shallow magma chambers fed the uppermost magma plumbing system of the CAP, hence resulted in its formation as nested igneous ring complexes through caldera collapse mechanism.

CHAPTER VI

CONCLUSIONS

Imaging of the Cretaceous CAP lithospheric structure in southern Malawi and northeastern Mozambique using aeromagnetic data and Bouguer gravity anomalies of the WGM 2012 showed that: (1) It represents nested igneous ring complexes made-up of two clusters (northern and southern) sourced for shallow (~4 km to ~6 km) magma chambers now frozen as broad batholithes. (2) It is underlain by thick crust where the Moho can be as deep as ~45 km. (3) It is underlain by thin lithosphere where the LAB can be as shallow as ~110 km. (4) The CAP was formed from a mantle melt sourced from decompression melting of the asthenosphere that ascended in response to NW-SE stretching of lithosphere during the Cretaceous during the Karoo rifting event. (5) Part of the ascended asthenospheric melt accreted at the base of the crust to form mafic magmatic under-plating body that resulted, in turn, in partial melting of the lower crust. The two magma sources mixed and rose to feed shallow magma chambers, which in turn fed the upper-most magma plumbing system of the CAP resulting in its formation through caldera collapse mechanism.

REFERENCES

Abdelsalam M. G., Liegeois J., Stern R. J. 2002. The Saharan Metacraton. Journal of African Earth Sciences 34,119-136.

Abdelsalam M.G., Katumwehe, A.B., Atekwana, E.A., Le Pera, A.K., Achang, M. 2016. The Paleoproterozoic Singo granite in south-central Uganda revealed as a nested igneous ring complex using geophysical data. Journal of African Earth Sciences 116, 198-212.

Ashwal L. D., Armstrong. R.A., Roberts R. J., Schmitz M. D., Corfu C F., Hetherington C.J., Burke K., Gerber M. 2006. Geochronology of zircon megacrysts from nepheline-bearing gneisses as constraints on tectonic setting: implications for resetting of the U-Pb and Lu-Hf isotopic systems. Contribution to Mineralogy Petrology 153, 389–403.

Avigad D., Gvirtzman Z. 2009. Late Neoproterozoic rise and fall of the northern Arabian–Nubian shield: The role of lithospheric mantle delamination and subsequent thermal subsidence. Tectonophysics 477, 217-228.

Azzouni-Sekkal, A., Liegeois, J-P., Bechiri-Benmerzoug, F., Belaidi-Zinet, S., Bonin, B. 2003. The “Taourirt” magmatic province, a marker of the closing stage of the Pan-African orogeny in the Tuareg Shield: review of available data and Sr-Nd isotope evidence. Journal of African Earth Sciences 37, 331-350.

Balmino G., Vales N., Bonvalot S., Briais A. 2012. Spherical harmonic modelling to ultra-high degree of Bouguer and isostatic anomalies. Journal of Geodesy 86, 499–520.

Baranov V. 1957. A new method for interpretation of aeromagnetic maps: Pseudo-gravimetric anomalies. Geophysics 22, 359-383.

Black R. Lameyre J. 1985. The structural setting of alkaline complexes. Journal of African Earth Sciences 3, 5-16.

Black R., and Liegeois J.P. 1993. Cratons, mobile belts, alkaline rocks and continental lithospheric mantle: the Pan-African testimony. Journal of the Geological Society150, 89-98.

Blakely R.J. 1996. Potential theory in gravity and magnetic applications. Journal of Applied Geophysics 36, 155-156.

Broom-Fendley S., Brandy E.A., Horstwood M.S.A., Woolley A.R., Mtegha J., Wall F., Dawes W., Gunn G. 2016. Quartz-Apatite rock from the Tundulu and Kangankunde Carbonatite Complexes, Malawi: Evidences for dissolution-precipitation of apatite and preferential LREE Mobility in late-stage hydrothermal process. American Mineralogist 101, 596–611.

Broom-Fendley S., Brandy E.A., Horstwood M.S.A., Woolley A.R., Mtegha J., Wall F., Dawes W., Gunn G. (2017). Geology, geochemistry and geochronology of the Songwe Hill carbonatite, Malawi. Journal of African Earth Sciences 134, 10-23.

Broom-Fendley., Brady A. E., Gunn G., Dawes W. 2017. REE minerals at the Songwe Hill carbonatite, Malawi: HREE-enrichment in late-stage apatite. Ore Geology Reviews. 81, 23-41.

Bloomfield, K. 1968. The pre-Karroo geology of Malawi. Memoirs Geological Survey of Malawi 4, 166 p.

Bloomfield, K. 1970. Orogenic and post-orogenic plutonism in Malawi. In: G. I. Clifford, T.N. (Ed.), African Magmatism and Tectonics. Oliver and Boyd, Edinburgh. 119-155

Bonin, B. 2007. A-type granites and related rocks: Evolution of a concept, problems and prospects. Lithos 97, 1-29.

Bonin, B., Ethien, R., Gerbe, M.C., Cottin, J.Y., Feraud, G., Gagnevin, D., Giret, A., Michon, G., and Moine, B. 2004. The Neogene to Recent Rallier-du-Baty nested ring complex, Kerguelen Archipelago (TAAF, Indian Ocean: stratigraphy revisited, implication for cauldron subsidence mechanisms. Geological Society of London Special Publications 234, 125-149.

Bonvalot, S., Balmino, G., Briais, A., M. Kuhn, Peyrefitte, A., Vales, Biancale, R., Gabalda, G., Moreaux, G., Reinquin, F., Sarraillh, M. 2012. World Gravity Map, 1:50,000,000. Editors: Bureau Gravimetrique International (BGI) – Commission for the Geological Map of the World (CGMW), Centre National d'Etudes Spatiales (CNES) – Institut de Reserche pour le Development (IRD), Paris.

Borradaile G.J. 1987.Anisotropy of magnetics susceptibility: Rock composition versus strain, Tectonophysic 138, 327-329.

Borradaile G.J., Henry B. 1997. Tectonic applications of magnetic susceptibility and its anisotropy. Earth-Science Reviews 42, 49-93.

Bouillin J et al., 1993. Granite emplacement in an extensional setting an AMS study of the magmatic structures of Monte Capanne (Elba, Italy) Earth and Planetary Science Letters 118, 263-279.

Boucheza J. L., Gleizesa G., Djouadia T., Rochette P. 1990. Microstructure and magnetic susceptibility applied to emplacement kinematics of granites: the example of the foix pluton (French Pyrenees). Tectonophysics 184, 157-171.

Bowden P. 1985. The geochemistry and mineralization of alkaline ring complexes in Africa (a review). Journal of African Earth Sciences 3, 17-39.

Broom-Fendley, S., Brady, A.E., Horstwood, M.S.A., Woolley, A.R., Mtegha, J., Wall, F., Dawes, W., Gunn, G. 2017. Geology, geochemistry and geochronology of the Songwe Hill carbonatite. Journal of African Earth Sciences 134, 10-23.

Burke, K., Ashwal, L., Webb, S. 2003. New way to map old sutures using deformed alkaline rocks and carbonatites. Geology 31, 391-394.

Crough S. T. 1983. Rifts and swells: Geophysical constraints on causality. Tectonophysics 94, 23-37.

Dill H.G. 2006. A review of mineral resources in Malawi with special reference to aluminum variation in mineral deposits. Journal of African Earth Sciences 47, 153–173.

Dixey F. 1937. The pre-Karoo landscape of the Lake Nyasa region, and a comparison of the Karroo structural directions with those of the rift valley. Journal of the Geological Society, London 93, 73 -93.

Dixey F., Bisset C., Smith W. 1955. The Chilwa Series of Southern Nyasaland: a group of alkaline and other intrusive and extrusive rocks and associated limestones. Geological Survey of Malawi Bulletin # 5, XXp.

Dowman E., Wall F., Treloar P. J., Rankin A. H. 2017. Rare-earth mobility as a result of multiple phases of fluid activity in fenite around the Chilwa Island Carbonatite, Malawi. Mineralogical Magazine. 81, 1367–1395.

Duraiswami R., Tahira S. 2014. Fluid-rock interaction in the Kangankunde Carbonatite Complex, Malawi: SEM based evidence for late stage pervasive hydrothermal mineralisation. Open Geosciences 6, 4.

Eaton D.W., Darbyshire F., Evans R.L., Grütter H., Jones A.G., Yuan X. 2009. The elusive lithosphere–asthenosphere boundary (LAB) beneath cratons. Lithos 109, 1-22.

Eby, G.N., Roden-Tice, M., Krueger, H., Ewing, W., Faxon, E., Woolley, A.R. 1995. Geochronology and cooling history of the northern part of the Chilwa Alkaline Province, Malawi. Journal of African Earth Science 20, 275-288.

Eby N.G., Woolley, A.R., Din, V., Platt, G. 1998. Geochemistry and Petrogenesis of Nepheline Syenites: Kasungu–Chipala, Ilomba, and Ulindi Nepheline Syenite Intrusions, North Nyasa Alkaline Province, Malawi. Journal of Petrology 39, 1405–1424.

Emishaw, L., Lao-Davila, D.A., Abdelsalam, M.G., Atekwana, E.A., and Gao, S.S. 2017. Evolution of the Broadly Rifted Zone in southern Ethiopia through gravitational collapse and extension of dynamic topography. Tectonophysics 699, 213-226.

Fairhead J., Okereke C. 1987. A regional gravity study of the West African rift system in Nigeria and Cameroon and its tectonic interpretation. Tectonophysics 143, 141-159.

Fritz, H., Abdelsalam, M.G., Ali, K.A., Bingen, K.A., Collins, A.S., Fowler, A.R., Ghebreab, W., Hauzenberger, C.A., Johnson, P.R., Kusky, T.M., Macey, P., Muhongo, S., Stern, R.J., Viola, G. 2013. Orogeny style in the East African Orogen: A review of the Neoproterozoic to Cambrian tectonic evolution. Journal of African Earth Sciences 86, 65-106.

Garson M. S. 1960. The geology of the Lake Chilwa area. Geological Survey of Nyasaland (Malawi) Bulletin # 12, XXp.

Garson, M. S. 1965. Carbonatites in southern Malawi. Geological Survey of Malawi Bulletin #15, XXp.

Gass I. G., Chapman D. S., Pollack H. N., Thorpe R. S. 1978. Geological and geophysical parameters of mid-plate volcanism. Philosophical Transactions of the Royal Society 288, 581-597.

Geyer A. Martí J. 2014. A short review of our current understanding of the development of ring faults during collapse caldera formation. Frontiers in Earth Science 2, 1-13.

Gómez-Ortiz D., Agarwal B., Tejero R., Ruiz J. 2011. Crustal structure from gravity signatures in the Iberian Peninsula, Geological Society of America Bulletin 123, 1247-1257.

Gómez-Ortiz D., Tejero-López R., Babín-Vich R., Rivas-Ponce A. 2005. Crustal density structure in the Spanish Central System derived from gravity data analysis (Central Spain). Tectonophysics 403, 131-149.

Goussi Ngalamo, J.F., Bisso, D., Abdelsalam, M.G., Atekwana, E.A., Katumwehe, A.B., and Ekodeck, G.E. 2017. Geophysical imaging of metacratonization in the northern edge of the Congo craton in Cameroon. Journal of African Earth Sciences 129, 94-107.

Hemanta K., Thébault E., Mandea M., Ravate D., Maus S. 2007. Magnetic anomaly map of the world: merging satellite, airborne, marine and ground-based magnetic data sets. Earth and Planetary Science Letters 260, 56-71.

Jacobsen B.H. 1984. A case for upward continuation as a standard separation filter for potential field maps. Geophysics 52, 1138-1148.

Johnson, S.E., Paterson, S.R., and Tate, M.C. 1999. Structure and emplacement history of a multiple-center, cone-sheet-bearing ring complex: The Zarza Intrusive Complex, Baja California, Mexico. Geological Society of America Bulletin 111, 607-619.

Ingram D.M., Causon D.M., Mingham C.G. 2003. Mathematics and Computers in Simulation. Mathematics and Computers in Simulation 61, 561-572.

Katumwehe, A.B., Abdelsalam, M.G., and Atekwana, E.A. 2015. The role of pre-existing Precambrian structures in rift evolution: The Albertine and Rhino Grabens, Uganda. Tectonophysics 646, 117-129.

Katumwehe, A.B., Abdelsalam, M.G., Atekwana, E.A., and Lao-Davila, D.A. 2016. Extent, kinematics and tectonic origin of the Precambrian Aswa Shear Zone in eastern Africa. Gondwana Research 34, 241-253.

Kröner A., Willner A., Hegner E., Jaeckel P. 2001. Single zircon ages, PT evolution and Nd isotopic systematics of high-grade gneisses in southern Malawi and their bearing on the evolution of the Mozambique belt in southeastern Africa. Precambrian Research 109, 257–291.

Macdonald R., Crossley R., Waterhouse K. S. 1983. Karroo basalts of southern Malawi and their regional petrogenetic significance. Mineralogical Magazine 47, 281-89.

Moreau C., Demaiffe D., Bellion Y., Boullierd A. M.1984. A tectonic model for the

location of Palaeozoic ring complexes in Aïr (Niger, West Africa). Tectonophysics 234, 129-146.

Morgan P. 1984. The thermal structure and thermal evolution of the continental lithosphere. Physics and Chemistry of the Earth 15, 107-193.

Morgan, W.J. 1972. Plate motions and deep mantle convection Memoir of the Geological Society of America 132, 7-22.

Neugebauer H. J., Reuther, C., Cognita T. 1987. Dynamic thermal thinning of the lithosphere and extensional tectonics. Terra Cognita 6, 320.

Neves S.P., Vauchez A., Archanjo C.J. 1996. Shear zone-controlled magma emplacement or magma-assisted nucleation of shear zones: Insights from northeast Brazil. Tectonophysics 262, 349-364.

Njinju, E.A., Atekwana, E.A., Stamps, D.S., Abdelsalam, M.G., Atekwana, E.A., Mickus, K.L., Nyalugwe, N. In Preparation. Lithopsheric structure of the Malawi rift: Implication for rifting processes in magma poor rift system.

O'Halloran D.A. 1985. Ras ed Dom migrating ring complex: A-type granites and syenites from the Bayuda Desert, Sudan. Journal of African Earth Sciences 3, 61-75.

Platt R.G, Woolley A.R. 1987. The mafic mineralogy of the peralkaline syenites and granites of the Mulanje complex, Malawi. Mineralogical Magazine 50, 85-99.

Platt R.G., Wooley A.R. 1986. The mineralogy of nepheline syenite complexes from the

northern part of the Chilwa Province, Malawi. Mineralogical Magazine 50, 597-610.

Pouliquen G., Connard G., Kearns H., Mohamed Gouiza., Paton D. 2017. Public domain satellite gravity inversion offshore Somalia combining layered-Earth and voxel based modelling. European Association of Geoscientists and Engineers 35, 73-79.

Ravat D., Pignatelli A., Nicolosi I., Chiappini M. 2007. A study of spectral methods of estimating the depth to the bottom of magnetic sources from near-surface magnetic anomaly data. Geophysical Journal International 169, 421–434.

Russo R.M., Speed R.C. 1994. Spectral analysis of gravity anomalies and the architecture of tectonic wedging, NE Venezuela and Trinidad. Tectonics 13, 613-622.

Rychert C.A., Shearer P.M. 2009. A global view of the lithosphere-asthenosphere boundary. Science 324, 495-498.

Rochette P., Jackson M., Aubourg C.1992. Rock magnetism and the interpretation of Anisotropy of magnetic susceptibility. Reviews of Geophysics. 31, 209-226.

Sarafian, E., Evans, R.L., Abdelsalam, M.G., Atekwana, E., Elsenbeck, J., Jones, A.G., Chikambwe, E. 2018. Imaging Precambrian lithospheric in Zambia using electromagnetic methods. Gondwana Research 54, 38-49.

Thybo H., Artemieva I.M. 2013. Moho and magmatic underplating in continental lithosphere. Tectonophysics 609, 605-619.

Tselentis G., Drakopoulos A. J., Dimitriadis K. 1988. A spectral approach to Moho

depths estimation from gravity measurements in Epirus (NW Greece). Journal of Physics of the Earth 36, 255-266.

Vail J.R. 1989. Ring complexes and related rocks in Africa. Journal of African Earth Sciences. 8, 19–40.

Viola,G., Henderson, I.H.C., Bingen,B., Thomas,R.J., Smethurst,M.A., deAzavedo, S. 2008. Growth and collapse of a deeply eroded orogen: insights from structural, geophysical, and geochronological constraints on the Pan-African evolution of NE Mozambique. Tectonics 27, TC5009. http://dx.doi.org/10.1029/2008TC002284.

Woolley A.R. 1987. Lithosphere metasomatism and the petrogenesis of the Chilwa Province of alkaline igneous rocks and carbonatites, Malawi. Journal of African Earth Sciences 6, 891-898.

Woolley A. R., Garson M. S. 1970. Petrochemical and tectonic relationship of the Malawi carbonatite-alkaline province and the Lupata-Lebombo volcanics. In: African Magmatism and Tectonics. T.N. Clifford and I.G. Gass (eds), 237-262.

Woolley A. R., Jones G. C. 1987. The petrochemistry of the northern part of the Chilwa alkaline province, Malawi. Geological Society of London, Special Publications 30, 335-355.

Zeng H., Xu D., Tan H. 2007. A model study for estimating optimum upward-

continuation height for gravity separation with application to a Bouguer gravity anomaly over a mineral deposit, Jilin province, northeast China. Geophysics 72, I45–I50.

VITA

Victor Nyalugwe
Candidate for the Degree of

Master of Science

Thesis: LITHOSPHERIC STRUCTURE BENEATH CHILWA ALKALINE PROVINCE IN SOUTHERN MALAWI AND NORTHEASTERN MOZAMBIQUE

Major Field: Geology

Biographical:

Education:

Completed the requirements for the Master of Science in Geology at Oklahoma State University, Stillwater, Oklahoma in May, 2018.

Completed the requirements for the Bachelor of Science in Geology at University of Malawi, Chancellor College, 2008

Completed the requirements for the Diploma in Education at Domasi Teachers Training College, Malawi, 2005

Completed the requirements for the Certificate in Education at Kasungu Teachers Training College, Malawi, 1994

Experience:

Boone Pickens School of Geology Graduate-Independent Studies (2015 – 2018).

Ministry of Natural Resources, Energy and Mining-Geological Survey Department

Ministry of education, Science and Technology Government High School-Geography (2008– 2013).

Professional Memberships:

National Association for The Black Geologists (NABG)
Society of Exploration Geophysicists (SEG)
American Geophysical Union (AGU)
Geological Society of America (GSA)
Forum for Malawi Geoscientists